Energy & Environmental Science

ROYAL SOCIETY OF CHEMISTRY

REVIEW

View Article Online
View Journal | View Issue

Cite this: *Energy Environ. Sci.*, 2025, **18**, 97

High-entropy materials for aqueous zinc metal batteries

Xiaomin Han, [a] Ran Zhao, *[a] Jingjing Yang,[a] Yahui Wang,[ab] Anqi Zhang,[a] Zhifan Hu,[a] Mengge Lv, [a] Chuan Wu *[ab] and Ying Bai *[ab]

Received 28th September 2024,
Accepted 30th October 2024

DOI: 10.1039/d4ee04442h

rsc.li/ees

To overcome the challenges raised by the utilization of intermittent clean energy, rechargeable aqueous zinc metal batteries (AZMBs) stand at the forefront due to their competitive capacity, low cost, and safety metrics. However, the side reactions at the anode, the instability of the cathode and the limited applications of aqueous electrolytes hinder its commercialization. High-entropy materials (HEMs), known for their multi-elemental composition and synergy, have shown great potential to alleviate the failure behaviors in various components, such as the electrochemical instability of electrodes, side reactions and electrolyte incompatibility with the reactive metallic anode. Based on the evaluation of emerging HEM strategies and the failure behavior analysis of AZMBs, this review discloses that the adoption of HEMs could be a universal solution to break the constraints in AZMBs and pave the way toward the development of high-performance AZMBs.

Broader context

Aqueous zinc metal batteries (AZMBs) have attracted widespread attention due to their significant advantages of low cost and high safety, making them one of the best candidates for large-scale energy storage. However, AZMBs face several challenges, including structural instability, cathode dissolution, zinc dendrite growth and side reactions during electrochemical reactions at the zinc anode, and a narrow electrochemical stability window of the electrolytes. To date, these dilemmas have not yet been fully overcome. In this case, high-entropy materials (HEMs) stand out due to their unique properties and functionalities, such as the pinning effect, lattice distortion effect, and cocktail effect. While specific electrode materials and electrolytes vary across different battery systems, the selection of key components in batteries generally follows some common principles and reaction mechanisms. Based on the significant progress made by HEMs in solving critical issues in LIBs or SIBs, this review examines the prospects of applying HEMs in AZMBs to address their failure behaviors and comprehensively enhance their performances. This review aims to bridge the applications of the high-entropy concept from existing rechargeable battery systems to AZMBs and offer innovative directions for the development of robust and practically feasible HEM-based AZMBs.

1. Introduction

The large-scale exploitation of fossil fuels coupled with the intensifying environmental deterioration have underscored the urgency of harnessing clean energy.[1] In this case, renewable energy sources hold significant importance in suppressing the increasingly severe energy crisis and catalyzing sustainable growth. Nevertheless, these energy sources usually show the characteristics of intermittent, unpredictable, and unstable power generation patterns.[2] To effectively utilize clean energy, these critical issues need to be given sufficient attention.[3] Battery technology for the storage of intermittent clean energy is regarded as an effective approach and has garnered significant attention. Within this emerging field, aqueous zinc metal batteries (AZMBs) have stood out due to their low cost and high security.[4] Due to their competitive theoretical capacity (820 mA h g^{-1} or 5855 mA h cm^{-3}), high crustal abundance, intrinsic safety, low standard potential (−0.762 V *vs.* SHE) and reversible stripping/plating, AZMBs have received much attention in recent years, and they are considered one of the best candidates for large-scale energy storage.[5,6]

Numerous research studies on AZMBs have emerged in an endless stream.[7] While the remarkable properties of AZMBs present outstanding development prospects, there are still many challenges in their practical applications.[8] Most prominently, similar to the phenomenon occurring in other battery systems, zinc ions tend to deposit on the anode inhomogeneously, which leads to uncontrollable dendrite growth and

[a] *Beijing Key Laboratory of Environmental Science and Engineering, School of Materials Science & Engineering, Beijing Institute of Technology, Beijing, 100081, China. E-mail: 6120230129@bit.edu.cn, chuanwu@bit.edu.cn, membrane@bit.edu.cn*

[b] *Yangtze Delta Region Academy of Beijing Institute of Technology, Jiaxing, 314019, China*

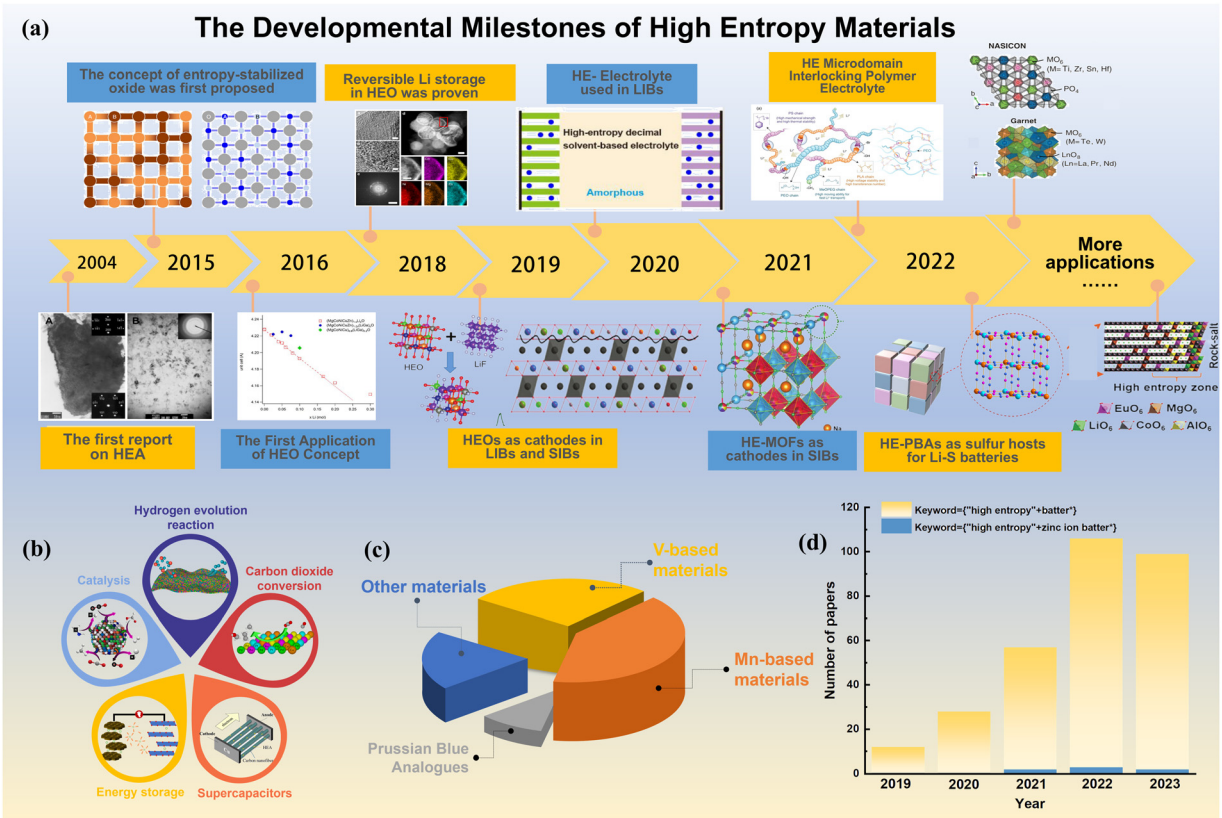

Fig. 1 (a) Developmental milestones of HEMs.[23–31] (b) Major applications of HEMs. (c) Publications of HEMs in the research of energy storage devices and zinc ion batteries (data from Web of Science). (d) Proportion of research papers on various cathode materials in AZMBs (data from Web of Science).

triggers the internal short-circuit.[9] The continuous side reactions, including corrosion, surface passivation and hydrogen evolution, result in an inferior coulombic efficiency (CE) and deteriorated performance, setting barriers to the real-world deployment of AZMBs.[10] Moreover, suitable cathode materials are still severely plagued by their limited selection.[11] The specific types and proportions of cathode materials used can be referred from Fig. 1(c). Cathode materials typically face several issues, as follows: (1) slow diffusion kinetics. The strong Coulomb interaction between Zn^{2+} and highly polar H_2O molecules forms hydrated $[Zn(H_2O)_6]^{2+}$. The large volume effect and the complicated desolvation at the electrode/electrolyte interface result in the slow migration of Zn^{2+} ions;[12] (2) structural collapse. The lattice spacing undergoes periodic expansion/contraction during the repeated ion insertion/deintercalation, inevitably leading to volume changes and structural pulverization;[13] (3) irreversible phase transition. Transition metals with d-electrons, such as Mn and Cu, are prone to induce the Jahn–Teller effect during the cycle process, which leads to distortion of the coordination of MO_6 from octahedron to quadrilateral;[14] (4) cathode dissolution. Transition metals undergo disproportionation reactions due to the Jahn–Teller effect, resulting in their dissolution in the electrolyte. Also, the acidic environment may accelerate the dissolution process.[15] The electrolytes in AZMBs also constrain their practical development.[16] Water as the solvent possesses a narrow electrochemical stable potential window (ESPW) of only ~1.23 V *vs.* SHE, restricting the practical energy density of AZMBs.[17] Moreover, owing to the high freezing point of water, AZMBs cannot be employed under low temperature conditions.[18,19] Zinc metal presents a high hydrogen overpotential and suitable standard potential, which make it suitable for direct use as an anode of AZMBs.[20] However, the hydrogen evolution reaction (HER) will spontaneously occur at the zinc anode/electrolyte interface based on thermodynamic aspects, elevating the local pH on the electrode surface, and thus facilitating the formation of by-products.[21] Furthermore, the gas evolution reactions increase the internal pressure and lead to the exhaustion of electrolyte. As a result, the cells show a decrease in both cycle durability and overall battery lifespan, and eventually damage the packed cells.[22] To date, various strategies have been proposed to solve these problems and optimize the electrochemical performance of AZMBs, but there is still room for improvement.

Fig. 1(a) illustrates the key milestones in the development of high-entropy materials (HEMs). Presently, HEMs are in the stage of rapid development and attract increasing interest.[23,32–35] HEMs usually refer to compounds containing five or more elemental components within a single-phase material.[36] Due to their unique structural characteristics, designable chemical composition and corresponding specific functions, HEMs have been widely applied in diverse areas of environmental science and renewable energy technologies (Fig. 1(b)).[37] The purpose of researching HEMs is to

develop advanced materials with unique performances. Remarkably, the progressive applications of HEMs provide a new research approach and have the potential to solve many problems that are difficult to break through in lithium ion batteries (LIBs),[38–40] sodium-ion batteries (SIBs)[24,41–45] and other systems.[46–49] Based on the unique properties of HEMs, such as pinning effect, cocktail effect, and lattice distortion effect, they can achieve a comprehensive performance improvement, resulting in fast ion transport dynamics, enhanced structural stability and reduced internal stress and/or strain accumulation in energy storage systems.[50–52]

Based on the significant progress using HEMs to solve critical issues in LIBs or SIBs, this review examines the prospects for the application of HEMs in AZMBs to address their failure behaviour and comprehensively enhance their performance. Firstly, this review clarifies the specific applications and elucidates the mechanisms of HEMs as components in LIBs and SIBs. HEMs can synthetically enhance the mechanical properties, thermal stability and cycle stability of the electrode materials. Through the cocktail effect and pinning effect, HEMs can mitigate problems such as oxygen loss, dislocation generation, volume expansion and harmful phase transformations happening in electrode materials. Electrolytes with high-entropy increase the ionic conductivity and broaden the operating temperature range of the electrolyte. By leveraging molecular or configurational diversity, these electrolytes significantly optimize the solvation structure and reduce ionic aggregation through entropic effects. After thorough analysis and careful judgment, we determined that although the specific electrode materials and electrolyte types vary across different battery systems within the energy storage field, the selection of key components in batteries generally adheres to common principles and reaction mechanisms. Furthermore, various energy storage systems encounter similar failure behaviors and mechanisms, such as phase transitions and structural instability in the cathode, dendrite growth and gas evolution reactions at the anode, and narrow operating voltage window for the electrolyte. The exploration of the high-entropy concept within AZMBs remains in its early stages. After comprehensively dissecting the specific application pathways and functions of HEMs for electrode and electrolyte modification in LIBs and SIBs, we can deduce that HEMs can eliminate the failure behaviour of the key components of AZMBs and address the common issues related to critical materials in batteries with similar structures and compositions. Additionally, the possible difficulties and challenges encountered in the potential application of HEMs in AZMBs are also analyzed by drawing on their comprehensive and basic understanding. This review aims to bridge applications ranging from the high-entropy concept existing in rechargeable battery systems to AZMBs and offer innovative directions for the development of robust and practically feasible HEM-based AZMBs.

2. Basic theory and synthesis of HEMs

The investigation of HEMs aims to delve deeper into the unexplored central regions of the multi-component phase diagrams and uncover unexpected synergies.[23,25,26] Precise regulation of the configurational entropy, which is achieved by altering the number and/or ratio of constituent elements, allows tuning of the phase composition and the adjustment of the intrinsic material properties.[27,33] The early investigations into HEMs date back to 2004, when Yeh first reported the field of metal alloys with high entropy and demonstrated their superior performance.[27,28] Since then, HEAs have been proven to be resistant to abrasion, corrosion and oxidation.[29] Following the success of HEAs, the concept of high entropy was extended to other compound types, broadening the scope of HEMs. The first HEO, extending the entropy concept to five-component oxides, was reported by Christina *et al.* in 2015.[23] The novel mixed oxides possess high configurational entropy and indeed remained entropy stable, which confirmed that the cations were distributed randomly and homogeneously. To date, the development of HEMs has been ongoing, encompassing a wide variety of compounds. These compounds include high-entropy alloys (HEAs),[27,28,30,33,46] HEOs,[24,31,53–58] high-entropy fluorides (HEFs),[59] high-entropy sulfides (HESs),[43,60] and high-entropy Prussian blue analogues (HEPBAs),[47] which have been explored for their potential applications in energy storage systems.

The definition of HEMs has two common manifestations, which are based on component composition and configuration entropy, respectively.[61] Introduced from the perspective of component composition, this definition first originated from HEA materials and refers to the fact that HEA materials are usually composed of five or more elements, each with an atomic ratio usually between 5% and 35%.[28,61] Subsequently, this concept transitioned from metal atoms to compound components. Hence, single-phase compounds containing five or more molecular compositions can also be generally referred to as HEMs.[53,62] Nowadays, HEMs are usually composed of one anion and multiple cations, and some studies also explored the composition of more than one type of anion.[63] Some studies proposed that five or more oxides with equimolar or non-equimolar ratios can be defined as HEOs.[25,53] This way to definite HEMs is also used in other compounds.[64] Significantly, regardless of the quantity of specific elements and phase number, HEMs with chemical disorder and structural order are usually single-phase compounds.[55,60]

The other way for defining HEMs emerged from the perspective of configuration entropy.[43,45,60,65] The material configuration entropy (S_{config}) can usually be calculated *via* the following equation:

$$S_{\text{config}} = -R\left[\left(\sum_{i=1}^{N} x_i \ln x_i\right)_{\text{cation}} + \left(\sum_{i=1}^{N} x_j \ln x_j\right)_{\text{anion}}\right] \quad (1)$$

where x_i and x_j represent the molar fractions of elements present in the cationic and anionic positions, respectively. R is the universal gas constant. S_{config} in the solid solution of component N (N = 2, 3, 4 or 5) represents a function related to the molar fraction of component N. Transitioning the focus towards compounds, particularly HEOs, it should be noted that the influence of potential oxygen vacancies is usually not considered because there is only one anion in HEO materials.[66] Therefore, the contribution of the anion sites will

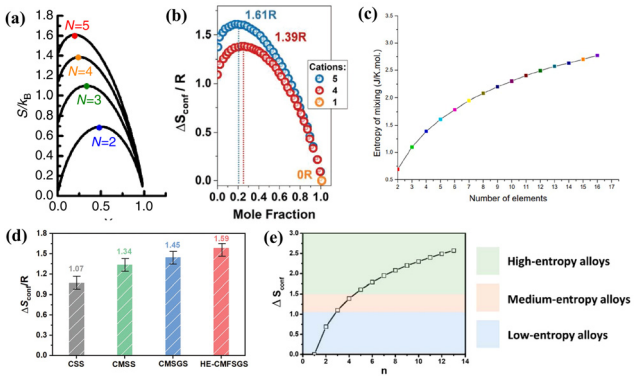

Fig. 2 Calculated configurational entropy of (a) HEOs;[23] (b) HE-PBAs;[45] (c) and (e) HEAs;[69,70] and (d) HESs.[43]

have little influence on S_{config} in HEOs. When modulating both the type and content of anions in other materials, the entropy of anions should also be considered in the calculation. When the materials are composed of different atoms, usually metal atoms, eqn (1) can be simplified to eqn (2), as follows:

$$S_{config} = -R\sum_{i=1}^{N} x_i \ln x_i \quad (2)$$

Based on the standard definition introduced, HEMs are defined as materials with a configuration entropy higher than 1.5R; materials with a value between 1.5R and 1R are classified as middle entropy; and materials with S_{config} lower than 1R can be determined as low entropy systems.[67] The value of S_{config} increases with the number of elements present in a given system. As illustrated in Fig. 2(a)–(e), entropy calculation and related trend analysis have been carried out in various studies. The maximum value of S_{config} can be calculated when the elements within a particular system have equal atomic proportions. The value of S_{config} can reach up to 1.61R in a five-cation system when each species component accounts for one fifth.[68]

HEMs have garnered significant attention due to their inherent capability and outstanding performance owing to the following four core effects.[30] These four core effects are shown in Fig. 3.

(1) High-entropy effects.[69,70] When mixing five or more elements to form large mixing entropy materials, HEMs tend to promote the development of a single-phase structure rather than a simple mixture of compounds.

(2) Lattice distortions.[43,61,71] Tremendous lattice distortion tends to emerge due to the different sizes of the doped atoms, depending on the atoms occupying these positions in the lattice and atomic types in local environments. These deviations introduce an intricate structure, which can influence the behavior of materials.

(3) Sluggish diffusion.[70] Predominantly manifested in HEAs, this effect elucidates the slow diffusion rates of the components in HEAs as opposed to that in stainless steels or pure metals. The phase equilibrium separation requires the cooperative diffusion among the components, which is obstructed by

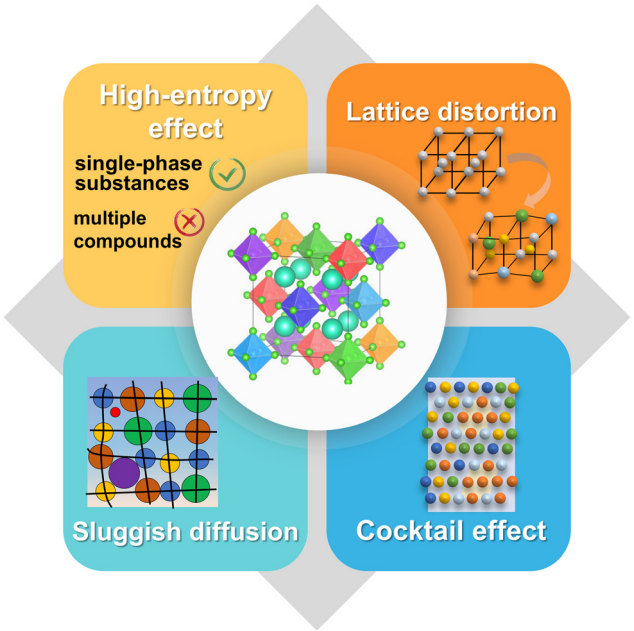

Fig. 3 Four common core effects in HEMs.

multi-components. Thus, the cooperative diffusion process becomes difficult.[72] The sluggish diffusion effect presents the possibility that the single-phase structure can maintain relative stability even in high-temperature and corrosive operating environments.[73]

(4) Cocktail effects.[61,74] The cocktail effect refers to the synergistic effect caused by the interaction between various elements, that is, a special combination of elements may produce the specificity of various properties. Generally, the cocktail effect explains the synergistic effect among these components, but the specific physical significance and how to promote a certain special property guided by linear laws are both still unclear.[25,37] Typically, the excellent properties in HEMs can be ascribed to the cocktail effect, such as near zero thermal expansion coefficient or catalytic response, ultra-high strength, good fracture toughness, fatigue resistance and ductility and other structural characteristics.[26,37,70] The appearance of cocktail effect mainly depends on the composition, microstructure, electronic structure and other characteristics of materials.[45,71]

The selection of the synthesis methods and the precise tuning of the reaction conditions are crucial for crafting high-entropy nanomaterials. By meticulously adjusting the synthesis parameters, HEMs with a controllable size, phase structure, and composition distribution can be produced.[75] The methods for the synthesis of HEMs are relatively straightforward, and generally follow routes similar to that used for traditional electrode materials. Taking the most commonly used materials in the energy storage field as an example, HEOs are mainly manufactured through solid-state reaction techniques.[76] Solid-state reaction methods involve the precise mixing of the precursor compounds in stoichiometric ratios, followed by mechanical grinding or ball milling, and then sintering at high temperatures to obtain the desired product.[77,78] The temperature and holding

time significantly affect the formation of single-phase materials. The solid-state reaction method is simple and easy to implement on an industrial scale, making it suitable for the large-scale preparation of HEOs. The sol–gel method involves dissolving metal alkoxides or salts to form a homogeneous sol, followed by a gelation process to produce solid HEOs. Solution combustion synthesis is also an effective method for synthesizing HEOs. This method involves the reaction of mixtures of various metal nitrates with glucose fuel, with short reaction times and the ability to synthesize homogeneous materials at lower temperatures.[57,79–81] HESs are typically synthesized through ambient temperature solid-state synthesis or traditional hydrothermal methods, with the precursors being multiple sulfide components.[43] The synthesis of HEPBAs mainly relies on co-precipitation methods, where multiple metal salts are mixed with hexacyano compounds in an aqueous solution to induce a precipitation reaction.[45,64,65] The processes of these typical synthesis methods are shown in Fig. 4.

The method for the preparation of liquid HE-electrolytes is similar to that of traditional electrolytes, involving mixing various different solutes or organic components into organic solvents or deionized water.[82] During the synthesis process, not only the solubility issue needs to be considered, but also the addition order and amount need to be precisely controlled. By stepwise addition, appropriate heating, and reasonable control of the molar ratio of components and solvent ratio, all the components can be uniformly dissolved and the electrolyte performance can be optimized. The synthesis method for solid HE-electrolytes can refer to the methods for the preparation of electrode materials. The synthesis methods used in existing research often involve high-energy ball milling, solution chemistry, sol–gel methods, and other methods to uniformly mix precursor materials, followed by high-temperature calcination to obtain solid HE-electrolytes.[83] The method for the mixing of the precursors refers to the physical and chemical properties of different substances. Usually, in the case of precursors that are easily soluble in solvents, the sol–gel method can be chosen to obtain solid electrolytes with better uniformity, while for metal oxides or nitrides that are not easily soluble, ball milling or solid-phase synthesis methods will be more appropriate.

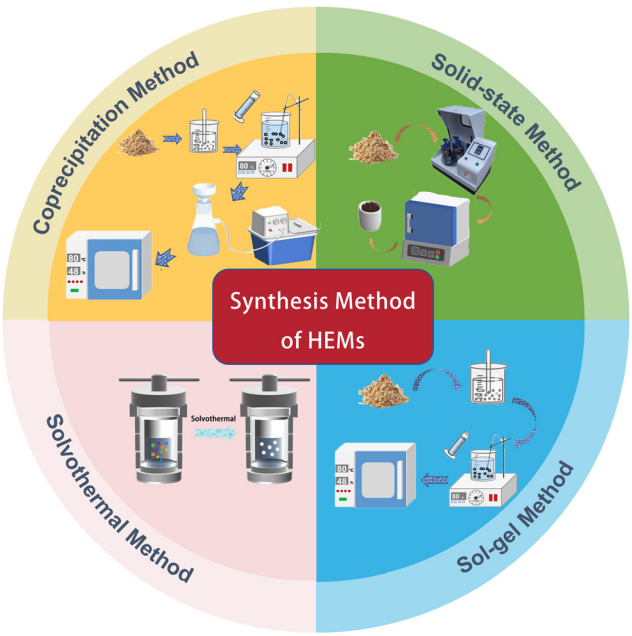

Fig. 4 Four common core effects in HEMs.

3. HEO cathodes with improved structural stability

The quest for energy storage systems with superior energy densities and stability has sparked extensive research on cathode materials with impressive performances.[84] The poor structural stability and narrow operating window of cathode materials in the current field of rechargeable batteries limit further application breakthroughs.[85] Introducing various elements into the lattice increases the configurational entropy, and the obtained cathodes combine the advantages of entropy configuration and doping effects, which can enhance the structural stability and effectively alleviate the lattice distortion caused by the Jahn–Teller effect.[61] This section delves into the specific applications of high-entropy cathodes in LIBs and SIBs, and then elucidates the relationship between composition and properties and extends this understanding to the design principles of cathodes for AZMBs.

3.1 HEM cathodes in LIBs

The most widely investigated cathode materials in LIBs include $LiCoO_2$, $LiMn_2O_4$, and $LiFePO_4$.[86] The rapid development of electric vehicles and portable electronic devices has led to an escalating demand for energy storage, which in turn fuels the relentless pursuit of enhancing the energy density of LIBs. Due to the high volatility of cobalt prices and geopolitical restrictions caused by the rare cobalt ore, many studies have been carried out on cobalt-free alternatives.[87] High-nickel cathodes, notable for their impressive energy density and cobalt-free composition, have garnered significant attention. However, in high-nickel cathodes, Ni^{2+} tends to migrate to the lithium layer and occupy the Li^+ site, leading to cation mixing between Li^+ and Ni^{2+}, which subsequently affects the extraction of Li^+.[88] An irreversible phase transition from the H2 to the H3 phase can easily occur during electrochemical cycles. This transition is accompanied by changes in lattice parameters and the generation of micro-stress, ultimately leading to electrode pulverization.[89] The timely introduction of the concept of high entropy offers a potential solution to these challenges. The $LiNi_{0.8}Mn_{0.13}Ti_{0.02}Mg_{0.02}Nb_{0.01}Mo_{0.02}O_2$ cathode, featuring high entropy, exhibited an unprecedented zero volume change during Li^+ intercalation and deintercalation, as illustrated in Fig. 5(a), and also achieved enhanced stability simultaneously (Fig. 5(b)), demonstrating a significant advantage over most cutting-edge high-nickel and low-cobalt cathodes.[35] The pinning effect is based on the high-entropy concept, which can reduce oxygen loss, avoid lattice expansion/shrinkage and prevent defect generation (Fig. 5(c)). Besides, the pinning effect

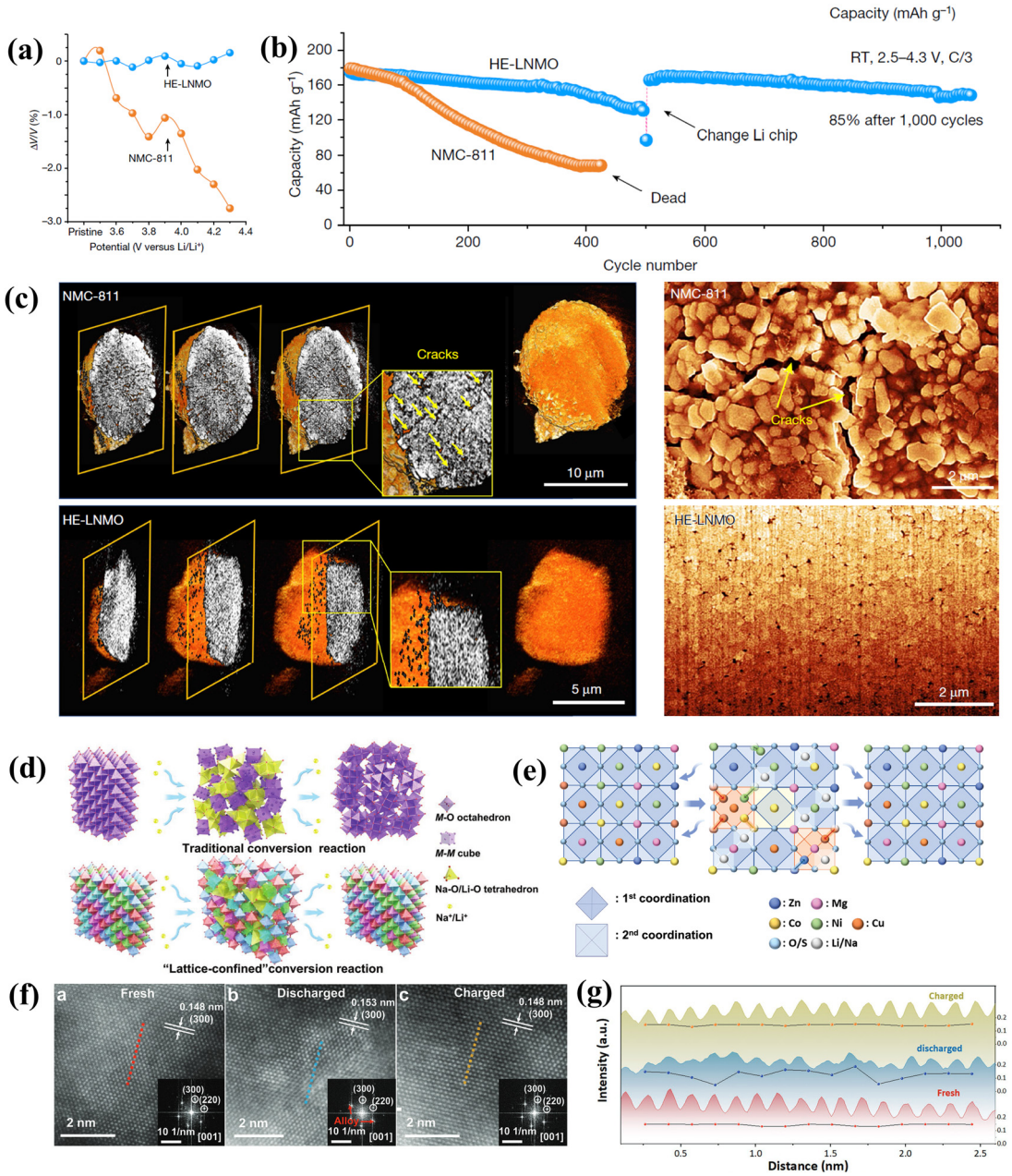

Fig. 5 (a) Volume change curves of HE-LNMO and traditional NCM811 cathode during the first charge. (b) Significantly optimized cycle life of HE-LNMO compared with NMC811. (c) Synchrotron-based TXM tomography (left) and cross-sectional SEM (right) images of NMC811 and HE-LNMO after long-term cycling.[35] (d) Schematic of the lattice-confined conversion reaction process. (e) Diagram of ligand environment change during the lattice restricted transformation reaction. (f) HAADF-STEM images of the HEOS in the fresh, discharged and charged states. (g) Intensity curve exhibits periodic changes.[89]

contributes to the structural stability even in both harsh long-term cycles and thermal abuse.

Conversion materials provide high capacity and low cost, but also face constraints due to their inherent structural instability, substantial volume changes, poor Li-storage reversibility, and limited cycle life.[90] The cocktail and pinning effects can effectively address the intrinsic challenges associated with conversion materials.[91] This synergy, achieved through a multifarious ionic framework, fosters the electrochemical properties of heightened stability. In this regard, HEFs, as conversion materials, have been proposed, demonstrating highly reversible lithium storage and enhanced Coulomb efficiency.[92] The addition or elimination of specific elemental constituents significantly influences the redox potential. Furthermore, materials subjected to high-entropy doping also manifest an obvious reduction in voltage hysteresis during electrochemical cycling.[61,77,92] It has been proven that HEMs present significant advantages in both capacity and voltage compared to medium-entropy materials, which are formed by reducing one element. This underscores the necessity for complex composition and meticulous element selection in HEMs. Moreover, HEMs also demonstrate an excellent performance in Li–S batteries. The

high-entropy perovskite oxide $La_{0.8}Sr_{0.2}(Cr_{0.2}Mn_{0.2}Fe_{0.2}Co_{0.2}Ni_{0.2})O_3$ (HE-LSMO) stands out due to its distinctive sulfur-infused porous fiber morphology, enabling its deployment as a sulfur carrier. A device based on HE-LSMO@S achieved a high specific capacity, remarkable rate performance and commendable cycling stability.[93] The incorporated metal elements can efficiently regulate the binding interaction of soluble polysulfides. The nanofibers, with their significant entropic contribution, serve as a bidirectional electrocatalyst between the soluble polysulfides and insoluble Li_2S during the liquid–solid conversion reaction.[48] HEAs are also cleverly used as key catalytic substrates to enhance the electrochemical capability of sulfur cathodes in lithium sulfur batteries.[46,94] Obviously, these alloy nanocrystals are strategically dispersed on nitrogen-doped carbon substrates, exhibiting significant electrocatalytic abilities. This helps to convert crystalline sulfur into the corresponding solid discharge residues through the soluble lithium polysulfide during the conversion process.

The regulation of anions in HEMs also results in outstanding electrochemical performances. Metal fluorides typically exhibit a higher electrochemical potential than oxides due to the strong ionic property of the M–F bond.[95] By incorporating fluorine ions into the lattice of HEOs, the working potential of LIBs increases to 3.4 V *vs.* Li^+/Li.[63] Concurrently, the stable entropy induced by the M–F bonds contributes to enhanced lithium storage properties and optimized cycle performance. As shown in Fig. 5(d), the integration of anions into the HEO framework can also be viewed as lattice-constrained conversion chemistry, which can prevent the structural collapse caused by stress localization and atom rearrangement in the conversion reactions.[96] By introducing sulfur and fluorine elements, and then forming HEOS/HEOF, respectively, the conversion reaction can be confined within the lattice framework during charge and discharge processes without significant phase changes and structural collapse. The sulfur/fluorine elements adjust the framework to accommodate lattice stress and inhibit atomic migration under the entropy stabilization effect (Fig. 5(f)).

3.2 HEM cathodes in SIBs

Cathode materials pose significant challenges to the rapid expansion of SIBs, given that they significantly lag behind anode materials and determine the energy density of the SIBs.[97,98] The common cathode materials in SIBs include transition-metal oxides (TMOs), polyanionic compounds and PBAs.[99] Among them, TMOs offer a higher energy density and the most mature preparation process, making them an important choice for commercial applications.[100] However, their low stability limits their practical application.[101] PBAs possess a high operating voltage, reversible capacity and significant cost advantage.[102] However, they are prone to defect formation and phase transition, leading to a decline in overall capacity and poor cycle stability.[103] Moreover, the technical threshold for the commercialization of PBAs presents a significant obstacle.[98] Polyanionic compounds exhibit high structural stability, long cycle life and high safety, but the development of polyanionic compounds is limited by their low specific capacity, poor conductivity, and challenges in large-scale production.[104,105]

Specifically, Na_xTMO_2 compounds have been extensively studied as cathode materials for SIBs, typically classified into O3, P3 and P2 types (P = prismatic, O = octahedral). P-type Na_xTMO_2 exhibits a superior rate performance and higher reliability than O-type Na_xTMO_2, owing to the larger residing sites for accommodating Na^+, reduced phase transition possibility, and faster ion diffusion kinetics in the trigonal prismatic environment.[106] However, after deep sodium deintercalation, P-type Na_xTMO_2 can easily transform into the detrimental P–O phase under high voltage charging conditions, harming the structural integrity and accelerating the capacity loss (Fig. 6(a) and (b)).[107] To inhibit this harmful phase transition, as shown in Fig. 6(c)–(e) and (l), the introduction of multiple metal elements into TM layers to achieve high-entropy has been proven to be an effective strategy. The pinning effect has also been demonstrated.[108] This effect not only can stabilize the structure and restrain the detrimental slab sliding and phase transition during the charge–discharge process, but also slow down the migration of cations from the TM slabs to Na layers, which can be confirmed by XRD during the cycle processes (Fig. 6(f)–(h) and (j)).[24,42,55,109] The phase transition can be divided into two parts during the cycle processes, *i.e.*, the O3 structure transforms to O3′ structure during the first charge process, followed by highly reversible phase transition behavior from P3 to the newly formed O3′ phase in subsequent cycles. The optimal diffusion paths of Na^+ in pristine P2, HE-P2, pristine O3, and HE-O3 cathode are presented in Fig. 6(i). The introduction of different metal elements generates multiple types of pinning centers within the materials, and the high-valence dopants present stronger interaction with the oxygen atoms, which can effectively pin the structure in place, making it more difficult for significant volume changes to occur.[110] The specific function of the pinning effect includes curtailing oxygen depletion, maintaining efficient pathways for ion and electron transport, limiting the growth and movement of detrimental phases or compounds and stabilizing the cathode structure during electrochemical reactions.[110,111]

The incorporation of electrochemically inactive dopants can further activate the redox reaction of oxygen, bringing the non-bonding O 2p band closer to the Fermi level after sodium ion intercalation.[112,113] Beyond the high-entropy effect, electrochemically inert Mg–O can prevent nanoparticle agglomeration through the bystander effect, thus maintaining the high reversibility of the active fraction.[114–116] However, the introduction of many inactive elements in HEMs results in discharge capacities that are lower than that of purely active materials. Thus, a balance must be achieved between enhancing the discharge capacity and ensuring a stable cycle life.[107]

The practical applications of PBAs are constrained by poor conductivity, inferior reversibility and low specific capacity, largely due to phase changes during the charge and discharge cycle.[117] As displayed in Fig. 7(a), the introduction of multiple elemental ions to achieve the high-entropy concept in the crystal structure of PBAs significantly enhances the structural stability and electrochemical properties, given that different

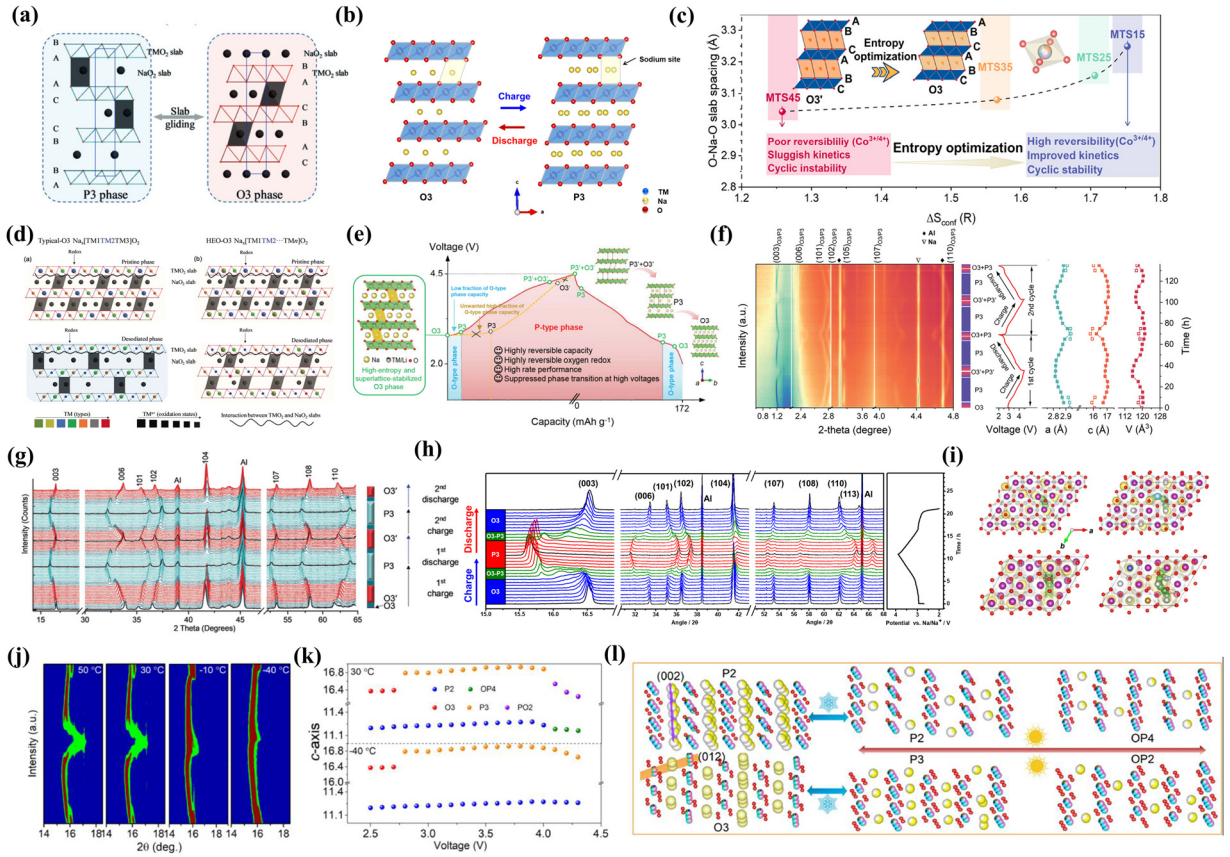

Fig. 6 (a) Crystal structure evolution of traditional layered oxides.[44] (b) Transition of the O3-type layered structure to the P3-type layered structure.[107] (c) Trend of O–Na–O slab spacing changes with configuration entropy in sodium deficient layered HEO.[107] (d) Possible structural changes in traditional layered oxides and layered HEOs after desodiating.[44] Schematic of crystal structure changes in layered HEO as cathode materials for SIBs (e) and *in situ* XRD patterns during sodium insertion/extraction (f).[42] (g) XRD patterns of an O3 layered HEO cathode for the first two cycles.[24] (h) XRD patterns and corresponding voltage curves of $NaCu_{0.2}Ni_{0.2}Fe_{0.2}Mn_{0.2}Ti_{0.2}O_2$ cathode.[55] (i) Optimal diffusion paths of Na^+ in pristine P2, HE-P2, pristine O3, and HE-O3 cathode. (j) Contour plots of *in situ* XRD spectra of layered HEOs at different temperatures. (k) Change curve of lattice parameters upon Na^+ extraction. (l) Schematic of structural evolution of P2/O3-NaMnNiCuFeTiOF.[109]

metal species share the same nitrogen coordination sites (Fig. 7(i)). With the unique cocktail effects formed synergistically by multiple elements, HEMs can stabilize the lattice and inhibit phase transitions (Fig. 7(b) and (h)).[45] There are differing perspectives on the phase transitions exhibited by HEPBAs during charge and discharge cycles. One perspective suggests that HEPBAs achieve a reversible transition through monoclinic–cubic–tetragonal phases (Fig. 7(c)).[118] HEPBAs exhibit a quasi-zero strain reaction mechanism (Fig. 7(d)), with the key to this improvement lying in the high entropy with correlation effects and the presence of several active redox centers.[65] Another viewpoint posits that the material only undergoes a highly reversible two-phase transition, not a three-phase transition.[119] Regardless of the specific phase transition mechanism, both viewpoints concur on the positive impact of high-entropy strategy on enhancing the lattice stability. Concurrently, theoretical calculations confirm that the Jahn–Teller effect of manganese elements is effectively suppressed, and the high-entropy strategy also enhances the bond strength of PBAs by increasing the integrated crystal orbital Hamiltonian population (ICOHP) values.[119] Based on different synthesis methods (Fig. 7(e)), the HEPBAs formed differ significantly in tap density and energy density, but there are significant advantages in both increased voltage plateau and cycle life (Fig. 7(f)). Besides, HEPBA also exhibits small voltage hysteresis and excellent energy efficiency (Fig. 7(g)).

The phase transition behavior of the pristine NVPF cathode at a low voltage plateau (≈3.4 V) could be mitigated by introducing other elements to design the HE-NVPF cathode (Fig. 8(a)).[120] This phase transition originates from the preferential intercalation of Na^+ at the Na(2) site during the charge and discharge processes. The high entropy effect could disrupt the occupation of the Na sites, suppress the rearrangement effect of the Na(2) site, and then inhibit the occurrence of the phase transition in the low voltage region (Fig. 8(e) and (f)). The average operating voltage was further increased to achieve the adequate storage of Na ions at high voltage platforms (Fig. 8(b)–(d)). As shown in Fig. 8(g), under the thermodynamic entropy gain and synergistic effect of multiple elements, HE-NVPFs also tend to form zero-strain materials.[121] When utilizing the HE-NVPF cathode, due to the existence of a high-entropy-assisted restraint mechanism, Na^+ can be fully retained within the potential

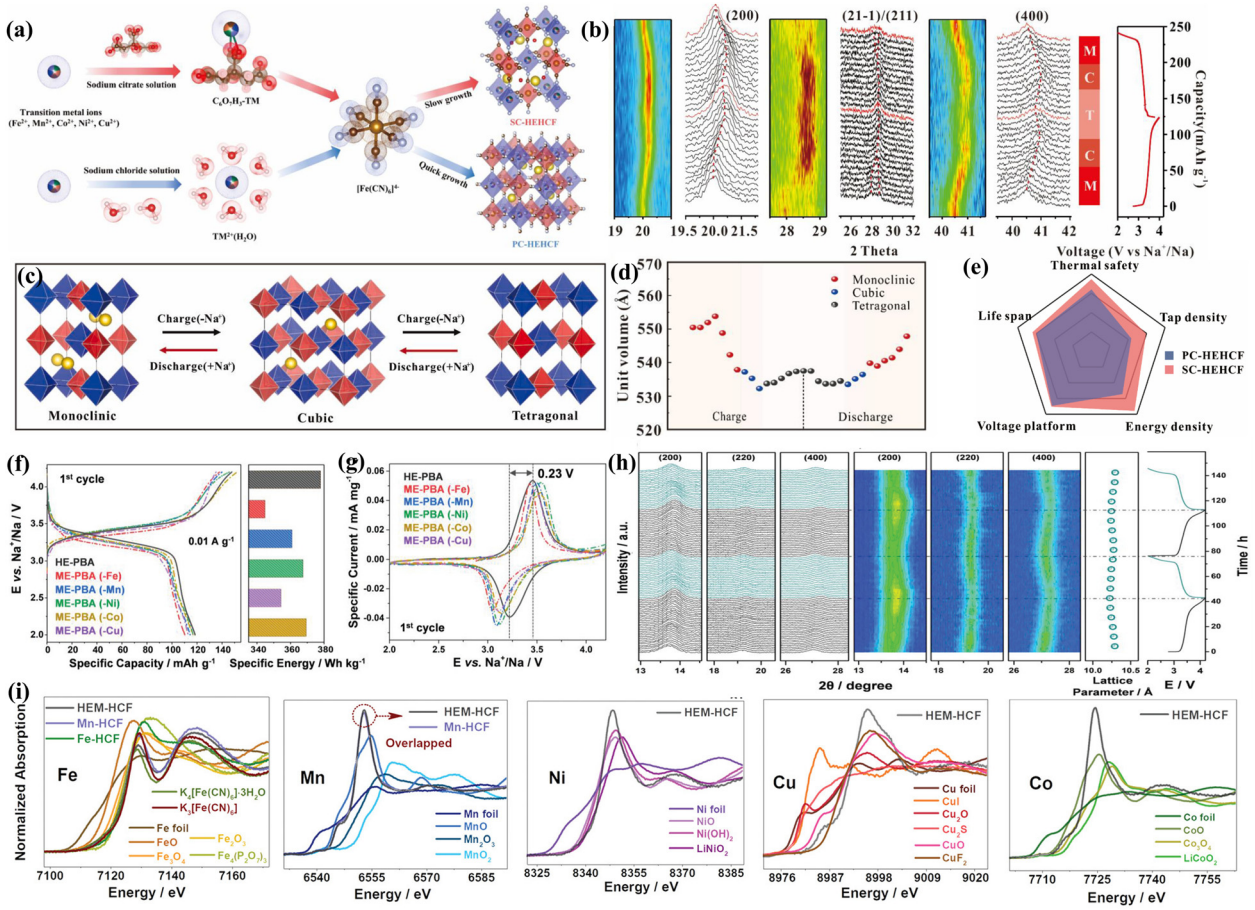

Fig. 7 (a) Synthesis process of a two-pronged approach of HE-PBA. (b) *In situ* XRD contour plot and representative reflection planes evolution of HE-PBA. (c) Diagram of the phase transformation of HE-PBA. (d) Unit volume of HE-PBA during the charge and discharge process. (e) Radar chart of two different synthesis speeds of HE-PBA based on physical and chemical properties and electrochemical performance.[118] (f) Charge and discharge curves of HE-PBA and different ME-PBAs at the first cycle. (g) CV curves for HE-PBA and different ME-PBAs. (h) XRD and the corresponding discharge/charge curves of the extraction/insertion of Na^+ into HE-PBA.[45] (i) XANES data of the elements in HE-PBAs.[119]

window, maintaining a high-voltage platform.[41] The solid-solution mechanism at low voltages can be observed in the HEM cathode. The theoretical calculation results confirmed that HE-NVPF has a smaller sodium ion migration energy barrier and lower band gap based on the lattice distortion effect, which can significantly improve the sodium ion migration kinetics and enhance the electronic conductivity of NVPF materials (Fig. 8(h)–(l)).[121]

3.3 HEM cathode in other systems

In the case of other energy storage systems, such as potassium-ion batteries (PIBs) and aluminum-ion batteries (AIBs), the insertion of large-volume or high-charge-density metal ions into the cathode inevitably leads to cathode volume expansion or structural collapse, resulting in a decline in cycle life. HEMs have also been preliminarily applied in key cathode materials for PIBs and AIBs.[122–124] The multi-component characteristics of HEMs can enhance the chemical and structural stability of materials, reducing the performance decline caused by volume changes during charge and discharge processes. The complex structure of HEMs may promote the rapid migration of high-charge-density ions, improving the rate of electrochemical reactions.

Manganese oxides, especially potassium ion pre-intercalated MnO_2 (KMO) cathodes, have great potential for energy storage in PIBs due to their high theoretical capacity, abundant raw material reserves, environmental friendliness, and low cost. However, the large radius of potassium ions causes significant volume changes in KMO cathodes during K^+ insertion/extraction. The KMO material also undergoes a P3–O3 phase transition during the K^+ extraction process, which affects the structural stability, leading to a rapid decline in capacity and limiting cycle life. The intrinsic low conductivity of KMO cathodes also affects the rate performance of PIBs. The introduction of HEM-based cathode plays a positive role in PIBs, especially in improving the ion transport, suppressing phase transitions, and enhancing the cycle stability. By introducing the high-entropy strategy into KMO (HE-KMO) cathodes, the harmful O3–P3 phase transition in KMO cathodes could be alleviated by effectively enhancing the covalent interaction between the transition metals and oxygen, and then reducing the structural stress changes caused by K^+ insertion/extraction (Fig. 9(a)). To date, two studies have already focused on HE-KMO cathodes, which could confirm this viewpoint, utilizing both theoretical calculations and *in situ* XRD

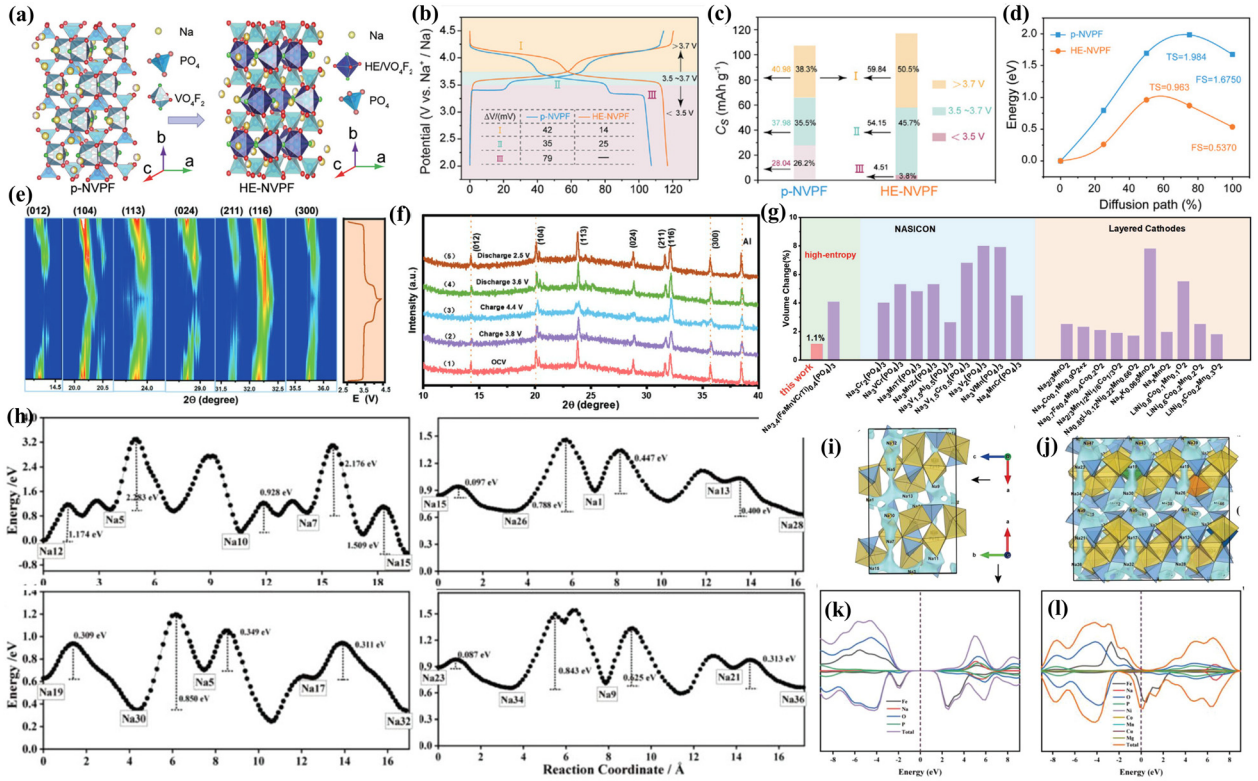

Fig. 8 (a) Configuration simulation of pristine NVPF and HE-NVPF. (b) Charging and discharging curves of pristine NVPF and HE-NVPF. (c) Discharge C_s values and capacity contribution rate of discharge voltage interval. (d) Corresponding migration energy distribution in pristine NVPF and HE-NVPF.[120] (e) Contour plot and corresponding voltage curve of HE-NVMP. (f) XRD patterns of HE-NVMP at different states. (g) Volumetric variation of HE-NVMP and other typical cathode materials.[121] (h) Migration energy barriers of Na^+ in pristine NFPP and HE-NFPP; Na^+ migration pathways of (i) NFPP and (j) HE-NFPP; DOS of (k) NFPP and (l) HE-NFPP.[121]

technology (Fig. 9(b) and (c)).[122,123] The local disordered structure caused by high-entropy doping allows the material to better accommodate stress changes during cycling, thus avoiding material dissolution and surface degradation (Fig. 9(d)). The HE-KMO cathode has achieved significant improvements in kinetics. From the perspective of electronic structure, the high-entropy strategy introduces a variety of transition metal elements. Through multi-element doping, the bandgaps of HE-KMO are narrowed, thereby enhancing the electronic conductivity. The introduction of multiple elements into KMO materials forms a locally disordered distribution of electron clouds. This local disorder not only disrupts the long-range ordered structure of the material but also creates more low-energy K^+ transport pathways between the layers, significantly reducing the energy barrier for K^+ transport and increasing the contribution of pseudocapacitive effects, allowing potassium ions to insert and extract more rapidly within the material, and thereby improving the rate performance of PIBs. Moreover, the reduction of the surface energy exposes more active (010) crystal faces (about 2.6 times more than low-entropy materials), which helps to enhance the K^+ diffusion and improve the reaction kinetics of the electrode.

The introduction of the high-entropy concept into the PBA cathode of AIBs has also resulted in a long cycle life and good rate performance.[124] As shown in Fig. 9(e), the high charge density of Al^{3+} inevitably leads to a large coulombic repulsion force during the electrochemical process, causing the severe structural degradation of conventional PBAs and poor long-term stability. In contrast, due to the doping of different atoms, the high-entropy effect and long-range disorder effect of HEPBAs give them a strong anisotropic lattice strain field. In the high-entropy structure, appropriate lattice expansion and contraction can greatly suppress the irreversible phase transitions. The situ X-ray diffraction test results show that the original PBA shifted to a higher degree during the discharge process, and excessive lattice changes led to stress accumulation and phase transitions (Fig. 9(f) and (g)). The initial displacement degree of the (200) and (400) crystal faces of HEPBA-Cu was low, and after a large number of discharge processes, it almost returned to the initial degree. The lattice change of HEPBA-Cu is similar to "breathing". After the introduction of high entropy, the strong distortion stress of the high-entropy material lattice causes the lattice to contract and return to the initial state. This "lattice breathing" effect of the HEPBA structure results in lower volume strain during cycling and enhances its cycle stability, as shown in Fig. 9(h).[124] At the same time, by synergistically mixing multiple metal elements, the intrinsic d-band expansion of metal elements in HEPBAs effectively regulates the local electron distribution, and the enhanced local charge compensation ability reduces the electron relaxation effect, achieving a better rate performance.

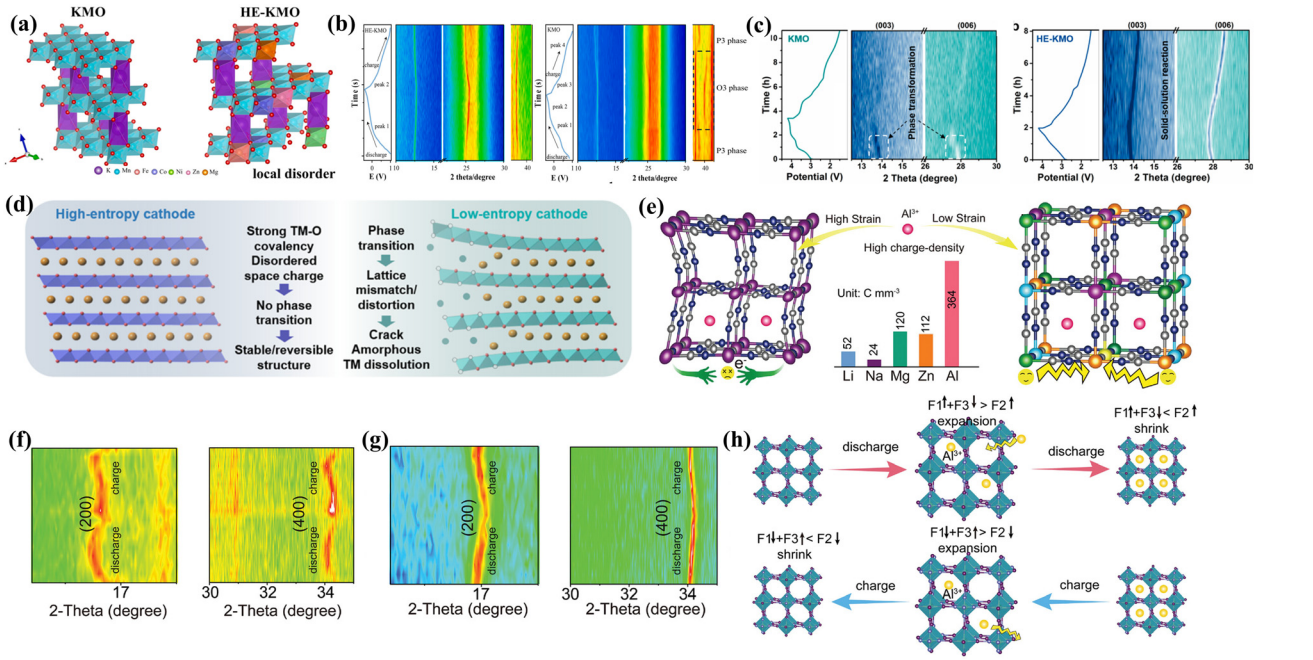

Fig. 9 (a) Schematic of the lattice structure of KMO and HE-KMO. (b) *In situ* XRD contour plot of HE-KMO (left) and KMO (right).[123] (c) *In situ* XRD patterns of KMO and HE-KMO electrodes at a current density of 20 mA g^{-1} in the wide voltage range of 1.5–4.2 V during the first cycle process. (d) Schematic of structural stability/failure mechanism of HE-KMO and KMO.[122] (e) Structural diagram of conventional PBA and HE-PBAs in AIBs. *In situ* XRD patterns of HEPBA-Cu (f) and conventional PBA (g) in AIBs. (h) Schematic of lattice changes of HE-PBAs during cycling process.[124]

3.4 Promising application prospect of HEM cathodes in AZMBs

As an emerging strategy, the application of HEMs in other rechargeable batteries offers multiple advantages by the pining effect, cocktail effect and lattice distortion effect, achieving cathode materials with superior stability, enhanced conductivity, improved tolerance to high voltage and higher capacity. Given that the failure mechanisms of rechargeable battery systems are very similar, such as unstable structure, harmful phase transition, low operating voltage, sluggish kinetics and byproduct formation, these existing findings in other systems suggest that the integration of HEMs can also stabilize the cathode materials of AZMBs and effectively address the existing challenges.

Despite the rapid progress in AZMBs in recent years, the lack of cathode materials that offer a stable cycle performance and high discharge specific capacity hampers their practical application.[125] The cathode materials in AZMBs include be PBAs, V-based materials, Mn-based materials and others, as demonstrated in Fig. 10. PBAs, as mentioned earlier, show a low reversible capacity and poor rate performance.[126] V-based materials show the merits of satisfactory specific power, but their fatal shortcomings need to be solved, including low operation voltage, low conductivity, dissolution behavior and high toxicity to humans.[127] Mn-based materials have been most widely investigated as cathode materials for AZMBs due to their low cost, moderate operating potential and numerous unique structural types.[128] However, the inevitable Jahn–Teller distortion originating from Mn-based materials manifests in the transition between Mn^{3+}/Mn^{4+} and Mn^{2+} generation during electrochemical cycles.[129] This phenomenon results in cathode dissolution, structural deterioration, and cycle performance degradation. The other types of materials usually show sluggish kinetics and structural instability, which are attributed to the intercalation of zinc ions with high charge density and large volume.[130]

Thus, to optimize the electrochemical performance of AZMBs, various strategies have been adopted, including defect engineering,[131] doping engineering,[73] pre-intercalation,[132] amorphization[133] and compositing with other materials.[134] However, these methods have certain limitations in improving their performance. Recently, a preliminary work was conducted using HEMs as cathode materials in AZMBs.[135] Benefiting from the cocktail effect (Fig. 11(a)), the HEO with five different metallic elements (Fig. 11(b)) achieved an optimized electronic structure and enhanced lattice strain field. The interaction of diverse types of metal atoms in HEOs resulted in a significantly broadened d-band and reduced degeneracy compared to monometallic oxides, which facilitated electron transfer and contributed to an exceptional rate performance (Fig. 11(c)).

Based on the successful applications of HEMs in rechargeable batteries and their intrinsic effects, it could be estimated that the HEMs possess broader application as cathode in AZMBs, and their potential effects are discussed in the following sections (Fig. 11(d)).

Enhancing the stability and extending the cycle life. The cathode materials in AZMBs, especially Mn-based and V-based materials, encounter significant challenges, such as structural instability and limited cycle lifespan.[136] Accordingly, one effective method to mitigate these challenges is metal ion doping, where the doped metal ions usually serve as structural pillars, establishing robust electrostatic interactions with the oxygen atoms within the lattice, reinforcing the interlayer bonds,

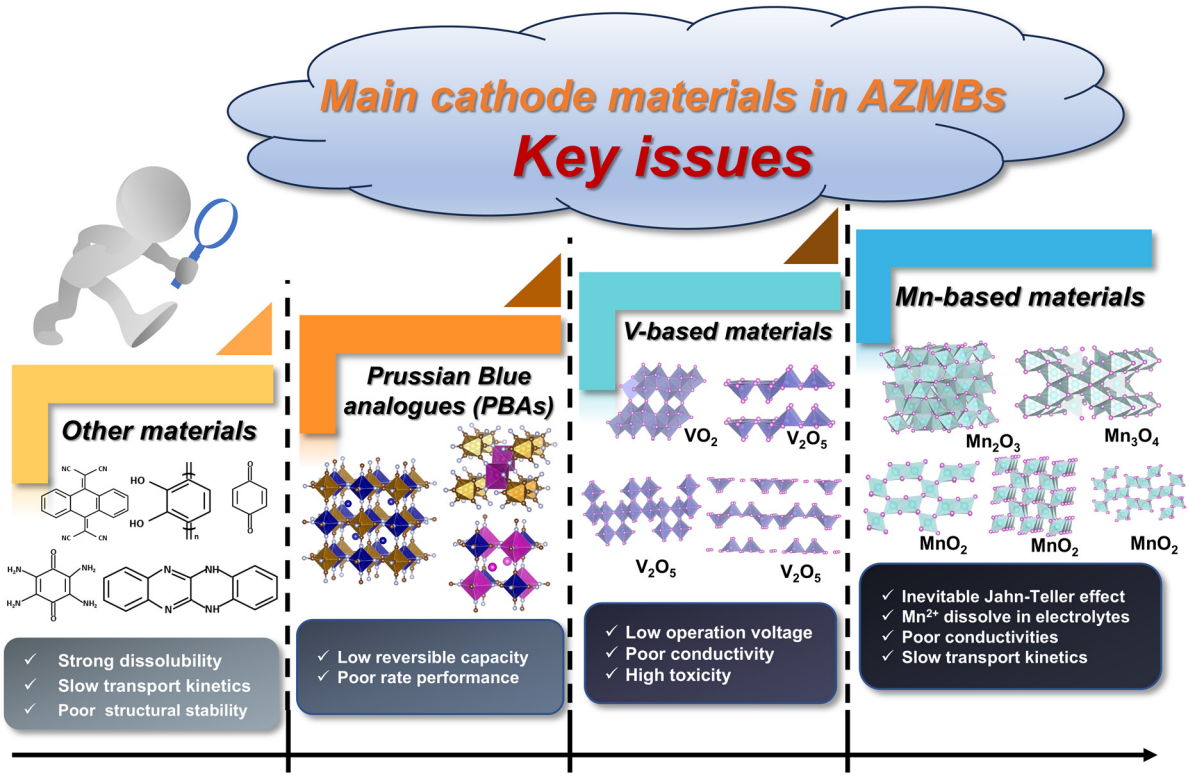

Fig. 10 Key issues in the existing cathodes in AZMBs.

effectively stabilizing the lattice and extending the lifespan of the electrochemical system.[137] Although the pre-intercalation strategy exhibits significant potential, there is still scope for improvement. The adoption of high-entropy components can achieve a comprehensive performance optimization. The unique pinning effect in HEMs is one of the key factors in improving their structural stability. The pinning effect refers to the significant lattice distortion and the complex local chemical environment caused by the presence of multiple metal elements.[138] These distortions and complex chemical environments can form potent pinning centers. (1) The random distribution of solute atoms within the materials and the interactions between different elements, such as size effects and elastic distortion effects, generate local stress fields. The pinning effect with local stress fields in high-entropy configurations inhibits dislocation slippage during ion intercalation and deintercalation across the crystal lattice. Due to the fact that the dislocations are pinned, the mechanical properties of the electrode materials are also enhanced.[123] (2) The close arrangement of different metal atoms tends to achieve the *in situ* confinement of the transition metal ions within the matrix structure. The synergistic pinning effect of multiple atoms contributes to the realization of zero-strain design, where the volume change in the material during the charge and discharge processes is minimized. This minimizes the structural damage caused by volume expansion or contraction, thereby significantly enhancing the cycling stability of batteries.[35] (3) The pinning effect appearing in layered HEMs can stabilize layered structures and maintain the integrity of the charge carrier migration pathways.[139]

Besides, each element in HEMs has a distinct valence electron configuration. The random distribution of these elements leads to the spatial mixing of their electron cloud structures.[140] This mixing can increase the overlap between electron clouds, potentially strengthening the metallic or covalent bonds, which in turn enhances the mechanical strength and chemical stability the of materials.[140] For example, the electron cloud between manganese and oxygen in Mn-based cathodes presents a denser overlap due to the interactions between the various metal elements, which enhances the bond energy of the Mn–O bond, making it less prone to breakage. The uniform charge distribution, facilitated by the presence of multiple elements, aids in reducing the localized electrochemical stresses, thereby enhancing the durability of the material.[43]

To achieve a high discharge specific capacity and enhanced lattice stability, it is crucial to carefully select and proportionally adjust various metal ions. Both the capacity and structural resilience can be optimized by precisely regulating the type and ratio of these ions, effectively utilizing the synergistic effect to elevate the performance threshold of the material.

Elevating the output voltage and increasing the energy density. To rapidly facilitate the practicality of AZMBs, it is vital to increase their energy density, which can be achieved by selecting materials with a superior theoretical capacity or high average discharge voltage. The high voltage plateau can be considered as a key parameter for attaining an improved energy density.

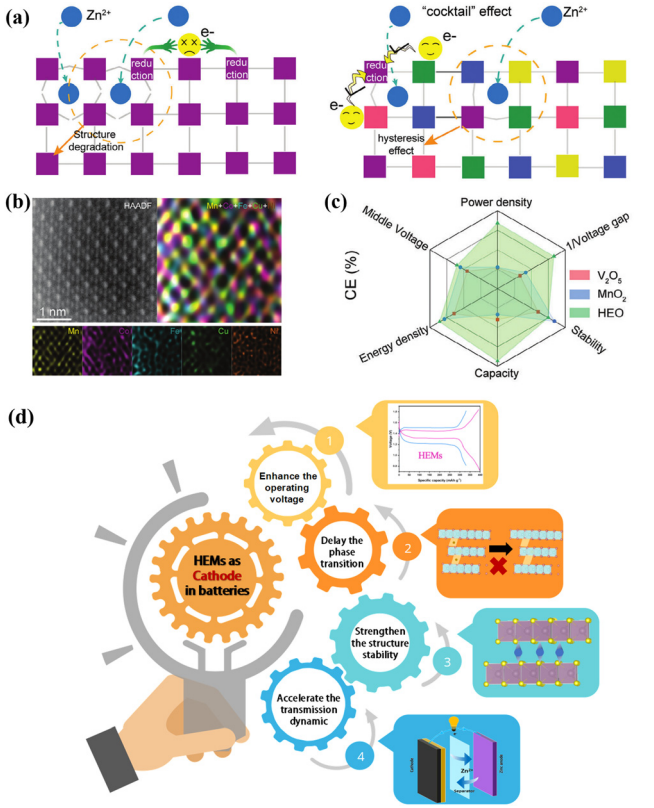

Fig. 11 (a) Schematic of traditional metal oxide electrode materials and high-entropy electrode materials with multiple electron paths in AZMBs. (b) EDS mapping of element distributions of HEM as cathode. (c) Radar maps based on HEM, conventional Mn- and V-based materials.[135] (d) Potential major advantages of HEMs as cathode materials for AZMBs.

For example, V-based cathode materials offer a higher theoretical capacity (generally exceeding 300 mA h g^{-1}, and even reaching up to 400 mA h g^{-1}), but suffer from a lower voltage plateau (0.9 V), which leads to a poor energy density.[141]

In this case, the adoption of the high-entropy strategy is beneficial to enhance the output voltage on the cathode side due to its multiple compositional and structural characteristics, which can be achieved by two pathways, *i.e.*, increasing the component entropy or structural entropy of cathode materials and introducing high entropy into the host materials or constructing a high-entropy interface layer between the cathode and electrolyte. (1) Firstly, the complex combination of elements in HEMs leads to the reorganization of their electronic structure at the microscopic level, which in turn alters the energy band structure of these materials, resulting in the formation of new bands or the broadening of existing ones.[142] This alteration in the band structure can have profound implications on the electronic and optical properties of materials. Adjusting the band structure can alter the electrochemical window of a battery, thereby affecting its discharge voltage.[143] (2) The enhanced structural stability of the bulk material and the interface, characteristic of high-entropy compositions, ensures material integrity over a broader voltage range, which can increase the electrochemical capacity contribution under high voltage.[110] (3) The diverse elements within these HEMs can undergo redox reactions at distinct potentials, contributing to an increase in energy density from a capacity perspective.[78] The above-mentioned arguments regarding the benefits of high entropy have been verified in various cathode materials, such as lithium cobalt oxide,[39] polyanion-type cathodes,[41] and Prussian blue.[45,144] These materials demonstrate a notable elevation in working potential following the introduction of high entropy.

Suppressing phase transitions and maintaining optimal reaction conditions. During the charge and discharge processes, cathode materials undergo phase transitions, which can lead to the instability of their crystal structures. This instability can result in their structural degradation, thereby reducing the reversible capacity and cycling stability of the battery.[145] Moreover, phase transitions may also induce alterations in the chemical properties at the surface of the cathode material, affecting the rate of carrier insertion and extraction reactions. For example, Mn-based cathodes, which are commonly used in AZMBs, frequently encounter significant phase transition issues. Within these Mn-based oxides, a mixture of Mn^{3+} and Mn^{4+} valence states exist. Mn^{4+} can form distortion-free [MnO_6] octahedra, contributing to stable crystal structures, but the high-spin Mn^{3+} tends to induce Jahn–Teller distortion. The valence state of Mn changes between +3 and +4 during the charge/discharge cycles.[146] This transformation causes the Jahn–Teller distortion to be repeatedly eliminated and reintroduced, leading to irreversible multi-phase transitions. Additionally, the vanadium in V-based cathode materials can exist in multiple oxidation states, and the transition between these states during battery operation can lead to phase changes, particularly in structures such as vanadium oxide. These phase transitions pose a considerable challenge to the practical application of these materials.[147]

Although the precise mechanism by which HEM cathodes suppress phase transitions has not been conclusively revealed to date, the effectiveness of HEM interface or bulk cathode materials in suppressing phase transitions could be elucidated from the fundamental theories.[42,122,148,149] (1) The disparity in the size and electronic properties of the constituent elements leads to a distribution of local stresses, which can hinder phase transitions at the microscopic level.[150] (2) A high mixing entropy contributes to stabilizing the disordered solid solution structure. The random distribution of multiple elements induces lattice distortion, which can impede long-range order within the lattice, thereby suppressing phase transformations.[151] (3) The dispersion in the electronic state of HEMs contributes to the stabilization of the lattice structure and reduces the electronic degrees of freedom within the lattice.[24] The interactions among different elements trigger the pinning effect, which can create a localized energy minimum value, stabilizing the lattice structure and inhibiting atomic or ionic mobility under thermal or electrochemical stimuli.[41,45] (4) An elevated thermodynamic stability, a typical characteristic of high-entropy systems, implies a lower free energy under specific temperature and pressure conditions, which further suppresses the tendency of phase transitions.[143] (5) Introducing high entropy at the cathode/electrolyte interface,

the robust interface confers additional stability and prevents phase transitions from the interface to the bulk. These viewpoints all indicate that HEMs possess the potential to suppress phase transitions effectively.[152] In brief, these properties endow HEMs and their interfaces with the capacity to effectively suppress phase transitions, thus enhancing their stability and applicability in various demanding applications, as well as in AZMBs.

Accelerating the transmission dynamics and optimizing the rate performance. HEMs profoundly influence the kinetics of materials through their unique compositional and structural characteristics. (1) Regarding electronic transport properties, the diverse elemental composition of HEMs potentially results in band structure modulation, thereby influencing the electron transport characteristics. The synergistic amalgamation of multiple metal elements broadens the density range of the intrinsic d-band center, while reducing the degeneracy.[152,153] This adjustment of the band gap, coupled with the complex local electronic states arising from the combination of various valence electron structures, can increase the electron scattering within the material, affecting the electron mobility rate.[142,154,155] (2) The distribution of stress and strain, resulting from differences in atomic sizes and chemical bonding, modifies the deformation behavior. Due to the complex diffusion pathways and lattice distortion caused by the intricate mixture of multiple elements with different sizes, HEMs can easily trigger localized strain within the lattice, which will affect the atomic migration kinetics and alter the diffusion behaviors.[154,156] (3) HEMs exhibit improved interface stability, which is crucial for controlling atomic and electronic transfer at the interface. The varying elemental interfaces may offer a range of distinct catalytic active sites, affecting the rate and pathways of chemical reactions at these boundaries.[157]

The complex behavior of material defects is significantly influenced by the unique characteristics of high entropy. For instance, the presence of oxygen vacancies is closely related to the elemental composition of materials. HEOs tend to generate more oxygen vacancies during their synthesis due to the presence of multiple elements with different valence states.[158,159] Both experimental results and computational models indicate that the vacancies introduced in HEMs can reduce the band gap in these compounds, and an increase in oxygen vacancies contributes to enhance electrical conductivity.[159] Besides, these oxygen vacancies provide additional active sites and cause imbalances in the charge distribution. The additional active sites are beneficial for increasing the specific capacity and imbalances in the charge distribution tend to create external coulombic forces, which facilitate carrier migration.[160] Recent advancements have explored the integration of vanadium ions into Mn-based oxides used in AZMBs, aiming to create a more extensive vacancy landscape.[161] This introduction not only can alter the electronic structure of traditional Mn-based materials, but also significantly improve the electric conductivity and enhance the diffusion kinetics of Zn^{2+}. This focus on the benefit of defect engineering in the synthesis of materials highlights the ongoing requirement to explore the use of HEMs as a method to introduce beneficial defects, thus advancing our understanding and capabilities in material design and functionality.

Looking back, the innovative incorporation of HEMs as components in cathode design has proven to be significantly effective across diverse electrochemical systems. Celebrated for their exceptional lattice robustness, the introduction of HEMs into AZMB frameworks perhaps leads to an enhancement in their comprehensive performance.

4. HEM anodes with enhanced reversibility

HEMs are regarded as anodes with great potential in the realm of rechargeable energy storage systems, which have been successfully applied in LIBs and SIBs. The high-entropy strategy can serve as a promising regulation method to alleviate the failure behaviors of the Zn anode in AZMBs. Its potential applications are presented as follows.

4.1 HEM anodes in LIBs

Metal lithium anodes, while offering high energy density, present significant safety issues in organic lithium-ion batteries. Consequently, the primary focus of research is alternative anode materials that can offer a balance between safety and high energy density. Transition metal oxides (TMOs) have emerged as potential candidates as LIB anodes. However, TMOs typically encounter issues such as low coulombic efficiency during the initial cycle, volume expansion, and poor conductivity.[162] Alternatively, disordered rock salts (DRXs) have gained recognition as promising anode materials, which achieve rapid lithium migration due to the permeable network provided by the octahedral–tetrahedral–octahedral pathway. Nonetheless, their rapid capacity decay and intricate charge storage dynamics have posed difficulties for the widespread application of DRXs.[163] Alloy anodes, formed by the combination of lithium with various metals, are expected to deliver extraordinary capacity, but alloying reactions frequently result in considerable volume expansion, resulting in significant strain during the electrochemical cycles. This strain can cause particle cracking, fragmentation, or pulverization, which in turn leads to a continuous reduction in capacity.[164] Conversion-type anode materials typically exhibit higher redox potentials during the charge–discharge processes and undergo significant volume changes during alloying or conversion reactions, which result in a reduction in overall working voltage and a diminished cycle life of the battery.[165]

Conventional binary metal oxides are usually two oxide compounds with different expansion coefficients to buffer the volume change in the conversion reaction. However, this enhancement is limited and still requires pre-structuring or combinations with conductive nanomaterials to achieve stable cycling. HEOs possess cations with different properties, leading to semi-coherent entanglement of the metal and oxide phases on the nanoscale, which provides an advantage over conventional bicationic oxides.[166] Similar to the applications of HEMs

as cathode materials, the distinctive characteristics of HEMs, notably the entropic stabilization effect, enhance the structural robustness and electrochemical stability of the anodes, thereby effectively alleviating the rapid capacity degradation typically encountered in rock-salt anodes.[167–170] The atoms/ions only need to locally align their positions along the well-defined lattice, which not only ensures a fast reaction, but also reduces the formation of Li_2O that leads to a capacity decline in the battery. All these factors help to protect the micron particles from fragmentation during the conversion and alloying reactions, giving the material an artificial pre-nanostructured behavior. This ultimately leads to a significant increase in the volumetric energy density of the electrodes and reduces the cost of industrial production. Entropically stabilized oxides have demonstrated outstanding capacity retention and reversible lithiation/delithiation behavior, maintaining their intrinsic rock-salt structure, while also serving as a stable host matrix for the conversion cycle.[167] Infusing inactive metal ions into TMOs is considered a viable method to improve their cycle performance; these ions act as pillars to reinforce the lattice structures.[171] The multi cation synergistic effect and cocktail effect of HEMs as anodes at the atomic and nanoscale in electrochemical reactions have been well validated.[172–174] Their excellent electrochemical properties are the result of the cation synergies, in which various metal elements can be combined to provide different functions. The mechanism for achieving a high discharge specific capacity in TM-HEO has been elucidated as a two-stage process. The initial stage involves the conversion of cations in the host material, for example, Cu^{2+}, Co^{2+} and Ni^{2+}, with the process initiated by Cu^{2+}. The subsequent stage involves conversion reactions, such as Mg^{2+} and Zn^{2+} ions, followed by an alloying/dealloying process. It is noteworthy that some elements undergo dual mechanisms for lithium storage, further demonstrating the intricate interplay among various components in the successful implementation of HEMs in battery technology.[175] Another view exists regarding the reaction mechanism, where during the first discharge, Li^+ ions migrate into the HEO particles, and the reduction of metal ions to the metallic state leads to a phase separation. (1) Some metal ions, such as Co^{2+}, Ni^{2+}, and Cu^{2+}, form simple face-centered cubic-structured alloys at the nanoscale throughout the micrometer-sized particles to form a 3D network; (2) some metal ions, such as Zn^{2+}, are further alloyed with Li to form an alloying nanophase; and (3) electrochemically inert metal ions, such as Mg^{2+}, maintain the oxide structure and act as a substrate to fill the metal network and accommodate Li^+ or Li_xO. After the first discharge, some of the metal ions, such as Cu and Ni, do not participate in the redox reaction, but maintain the backbone of the nanoscale three-dimensional metal network with good electronic conductivity.[174] The micrometer-sized material particles are transformed into composites with an intrinsic semi-common-lattice metal/oxide nanophase.[166]

The key physicochemical properties of HEMs, such as their electronic structure, geometric configuration, and surface adsorption, can be fine-tuned through the rational and controlled introduction of defects. The viability of introducing defects has been demonstrated through various techniques, including ion doping,[160] the creation of oxygen vacancies,[176,177] acid etching,[178] and plasma treatment.[179] For instance, the targeted introduction and regulation of oxygen vacancies in the rock-salt type (MgCoNiCuZn)O anode of LIBs using a wet chemical molten salt strategy can significantly enhance the conductivity by accelerating the ion and electron transport. This approach also provides additional active sites, increasing the surface capacitance. Both experimental results and theoretical calculations indicate the potential for the improvement in lithium storage, charge transfer, and diffusion kinetics through HEO surface defects, ultimately enhancing the electrochemical properties.[180]

The introduction of the high-entropy strategy into spinel-type anodes is also an effective modification method. Anodes with a spinel phase consistently demonstrate superior Li storage capacity compared to that with a rock-salt structure. By incorporating the high-entropy approach to construct spinel-type anodes, multi-stage Li storage behavior emerges (Fig. 12(a)).[77] Li^+ also undergo conversion reactions in high-entropy spinel-type anodes, forming a multiphase state composed of various metal phases and Li_2O phases. This behavior serves as an effective countermeasure against the adverse effects of volume expansion and the resulting electrode pulverization.[78] The coordination and integration of various metal cations with different radii, valence states and reaction potentials, coupled with the entropy stabilization effect, endows spinel-type HEMs with enhanced reversible cycle durability and excellent electrochemical performance as anode materials in LIBs. As shown in Fig. 12(f), during the cycling process, reversible phase transformations within the spinel phase and reconstruction of crystalline domains occur. Both the transition metals and generated lattice oxygen participate in the charge compensation, contributing to the reversible capacity (Fig. 12(g)).[181] Doping more elements into the high-entropy M_3O_4 dramatically changes the static charge distribution, providing more free electrons for electron transport, as well as altering the local chemical order, resulting in a more stable molecular structure and higher electronic conductivity at the negative electrode.[181] By substituting pristine Ni with Mg elements in spinel-type HEO anodes, high capacity and excellent stability are obtained.[180] Based on the medium-entropy $(CrNiMnFe)_3O_4$, HEMs were formed after introducing different fifth elements (Fig. 12(d) and (e)), presenting diverse discharge ability and cycle reversibility, which can be attributed to the differences in oxygen vacancy concentrations resulting from the distinct elemental compositions.[81] Moreover, as shown in Fig. 12(c), the surface modification of HEMs has been proven to increase their total specific surface area and improve their transport dynamics.

Fluorides, known for their strong ionic bonding and high electrode potential, often undergo irreversible lattice structure transformations after the initial lithiation. Thus, high-entropy perovskite fluorides (HEPFs) have been designed to effectively address this issue, featuring a unique three-dimensional cubic framework structure (Fig. 12(b)).[182] The synergistic effect between the high entropy and the multiple redox-active centers in HEPFs is crucial for optimizing their performance. It has

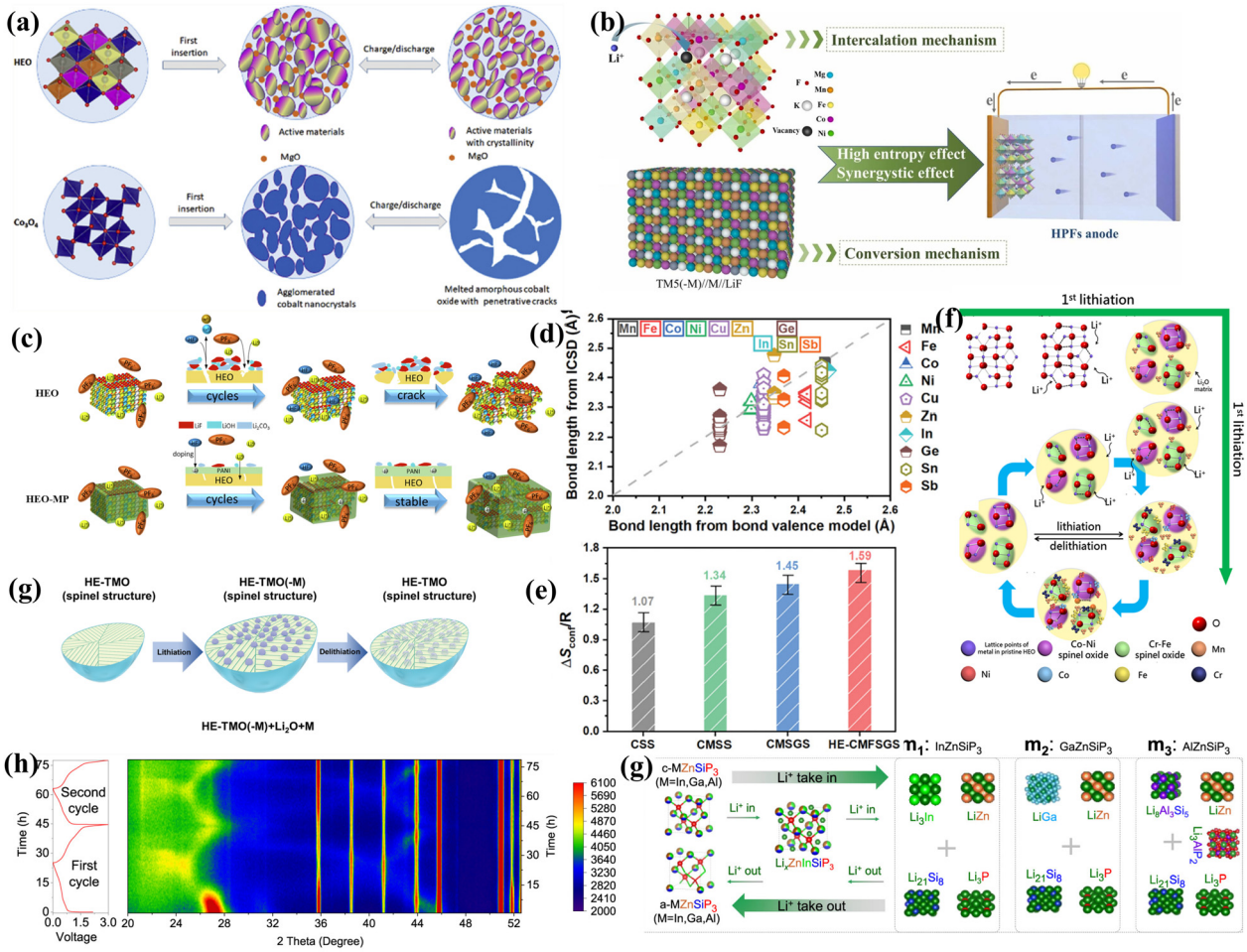

Fig. 12 (a) Schematic of cycling mechanisms of HEO and Co_3O_4 materials used as anodes for LIBs.[77] (b) High-entropy effect and synergistic effect of HEPFs.[182] (c) PANI interface on the HEO surface facilitates the inhibition of side reactions.[81] (d) Bond length calculated from bond valence model. (e) Calculated configurational entropy for different compositions.[43] (f) Schematic of the evolution of the atomic-scale microstructure of HEO during the cycling process.[181] (g) Illustration of lithiation/delithiation mechanism with the conversion reaction of HE-TMOs as anode of LIBs.[181] (h) Lithium storage mechanism of In (or Ga or Al) $ZnSiP_3$ silicon-based compounds. (i) Schematic of the generalized reaction mechanism of In (or Ga or Al) $ZnSiP_3$.[183]

been confirmed that only a portion of metal ions participate in the electrochemical reaction at the TM5 electrode during complete discharge, while the remaining metal ions play a crucial role in its structural stability.

Silicon-based anode materials for LIBs offer significant advantages such as high theoretical specific capacity, low operating voltage, abundant resource availability, and low cost. However, they also face challenges such as severe volume expansion during the charge and discharge processes and poor intrinsic electronic and ionic conductivity. In this case, introducing the high-entropy concept into silicon-based anodes can improve their electrical conductivity and ionic diffusivity, enhance their structural stability, and suppress side reactions through multi-element phase reactions. The high-entropy strategy introduces a variety of elements, reducing the bandgap width and increasing the electronic state density, which significantly enhance the electronic conductivity, especially near the Fermi level. The results of experiments and theoretical calculations have shown that high-entropy silicon-based compounds exhibit lower migration barriers for Li^+ ions and higher Li^+ diffusion coefficients, facilitating rapid charging and discharging processes. Among the high-entropy silicon-based compounds, $InZnSiP_3$ demonstrates the highest Li^+ affinity, the fastest electron conduction and Li^+ diffusion, the highest lithium storage capacity and reversibility, and good mechanical flexibility.[183] By forming more complex lattice structures, high-entropy silicon-based compounds have better resistance to volume expansion during the charge–discharge cycles, reducing the pulverization of the electrode caused by the lithium insertion/extraction process, and thereby improving cycle stability (Fig. 12(h)). The introduction of multiple elements in high-entropy silicon anodes creates more local disorder and structural defects, which help to disperse the stress from Li^+ insertion and extraction, suppressing phase transitions and structural degradation of the silicon electrode during cycling. As shown in Fig. 12(i), the introduction of multiple elements and the formation of complex electrochemical intermediates during the reaction process can effectively suppress the

occurrence of side reactions on the material surface, enhance the coulombic efficiency, and extend the electrode life.

The high-entropy concept serves as inspiration to expand the basic elements to alloy anodes, thereby avoiding volume expansion and bolstering the reversibility. The configuration entropy values of HEAs increase and overcome the enthalpy of compound formation, which suppresses the occurrence of potentially undesired additional intermetallic compounds.[184] For instance, an atomically disordered HEA composed of Ge–Sn–Sb–Si–Fe–Cu–P exhibited high reversibility, suitable discharge potential and large discharge capacity.[185] As displayed in Fig. 13(a), HEA nanoparticles were greatly embedded and encapsulated into a carbon matrix to form a dragon-fruit-like HEA/C composite, which also showed an improved performance. The reaction mechanism, as shown in Fig. 13(b), suggests that some of the elements (Ge, Sn, Sb, Si, and P) contribute to the Li storage capacity, while the remaining elements (Fe and Cu) bridge the fast electronic connection across the electrode. The binary Y_5Sb_3 compound was partially substituted with elements such as Pr and Sb to form alloys with high entropy and the general formula $Y_{5-x}Pr_xSb_{3-y}My$ (M = Sn, Pb), and this HEA showed a highly disordered phase.[186] The insertion of Li/Na into the octahedral gap promotes the formation of highly disordered high-entropy intermetallic phases during the electrochemical lithiation process. After modifying this HEA with CNTs, the composite achieved a higher discharge capacity and an extended cycle life.[186] The cocktail effect of different constituent elements results in the existence of multiple Li^+ transport pathways and abundant active centers in HEAs (Fig. 13(c)).[187] The active centers with gradient absorption energy reduce the local current density and nucleation overpotential on the anodic surface, promoting selective binding and providing a low potential barrier for uniform Li nucleation (Fig. 13(e)). Multiple transport pathways facilitated the Li^+ diffusion behavior, resulting in uniform Li deposition (Fig. 13(d)). The lithophilic sites of HEAs reduced the surface tension of the Li metal nuclei and formed a uniform SEI layer on the lithophilic surface, which greatly contributed to the homogeneous dispersion of Li nanoparticles across the HEA/C surface.

The examples mentioned all confirm the successful application of HEMs as anode materials in LIBs, including rock-salt type anodes, spinel-type anodes, conversion anodes and alloy anodes. HEM anodes can not only the improve structural stability of various anode materials, but also enhance their ion transport kinetics and cycle life.

4.2 HEM anodes in SIBs

The research on HEMs for improving the anode materials in SIBs remains in a relatively early stage, which was only presented in two investigations of oxide and sulfide.[43,188] The mechanical stress from transition metal sulfides (TMSs) accumulated during the cycling process may lead to persistent fracture of the SEI film and anode pulverization, leading to a low CE and unexpected capacity degradation. In this case, some approaches, such as hollow structures, introduction of layered carbon skeletons and phase engineering of heterogeneous interfacial structures, have yielded encouraging electrochemical results.

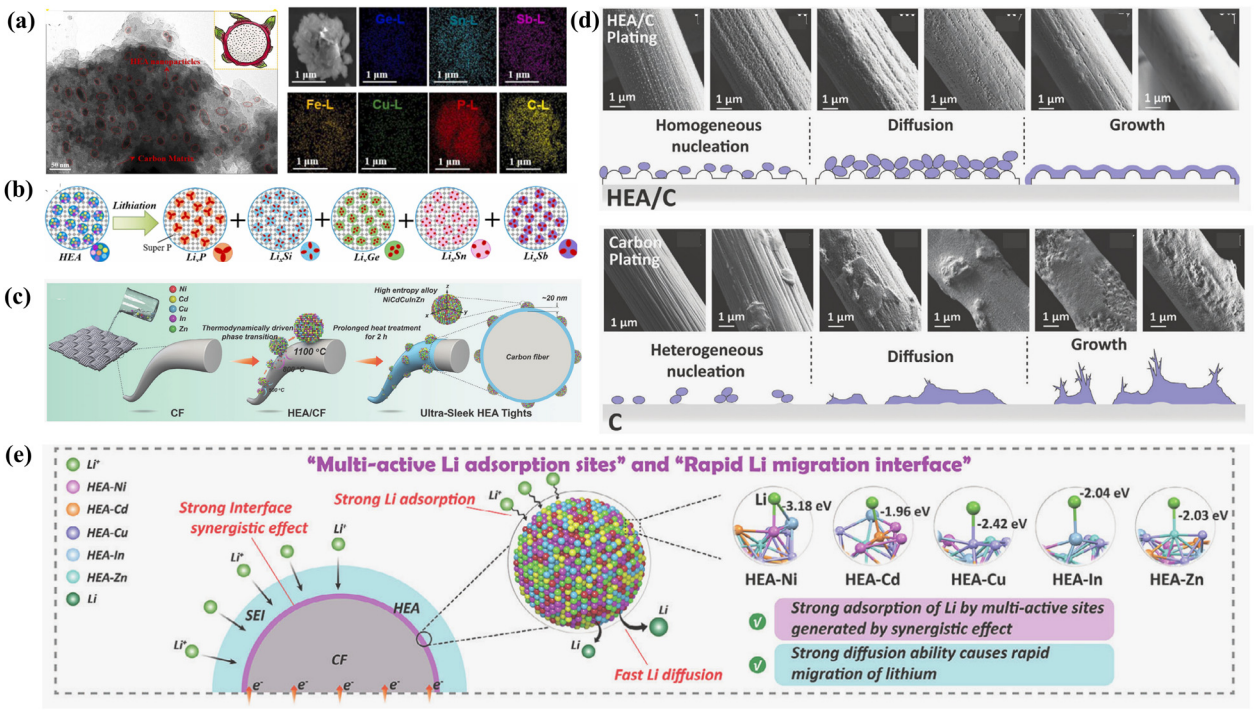

Fig. 13 (a) SAED image and elementary mapping of HEA/C composite. (b) Multi-alloying reaction mechanism of HEA/C composite.[185] (c) Schematic of the preparation processes of the ultra-sleek HEA tights. (d) SEM images of lithium deposition morphology on HEA/C and C host surface and schematic of lithium deposition on HEA/C and C hosts. (e) Schematic of Li adsorption and diffusion over HEA/C.[187]

However, nanocrystal aggregation and structural collapse still occur in subsequent cycles.[189] By adopting a high-entropy configuration strategy in TMSs, the anode can achieve high electronic conductivity and multiple electron transfer reactions facilitated with near-metallic compounds.[43] The innovative combination of the two concepts of high entropy and reduced material size has resulted in excellent material properties. The uniformly dispersed cations effectively suppress the continuous coarsening of the Sn nanoparticles and maintain effective interfacial contact between M^0 and Na_2S, potentially leading to highly reversible sodium storage. The most obvious advantage is the highly reversible crystalline phase transition and inherent strong mechanical stability achieved by HEMs, which effectively alleviate the continuous accumulation of mechanical stress. Multiple immiscible metal oxides were controllably doped into sub-1 nm nanowires using polymetallic oxide clusters, and in this process, the metal oxide and polyoxometalate (POM) species could be flexibly tuned. The resulting synthetic HEO-POM SNWs achieved a high degree of structural order and improved electrochemical performance due to the entropy modulation effect.[188]

4.3 Application of HEM as anodes in AZMBs

Notably, metal zinc, with its favorable standard potential (−0.76 V *vs.* SHE), low cost and substantial theoretical capacity (820 mA h g^{-1}, 5854 mA h L^{-1}), has become the dominant anode of choice in contemporary AZMBs.[190,191] However, several challenges hinder the practical application of AZMBs, including dendrite growth, gas evolution, and passivation.[192–194] The intractable issue of Zn dendrite growth in AZMBs largely originates from the heterogeneous electric field and ion flux distribution.[195,196] After nucleation, during the two-dimensional diffusion process, zinc ions, similar to lithium ions, experience a tip effect and preferentially continue to react at sites of high curvature, inducing the formation of dendrites.[197] Eventually, they can pierce the separator, leading to a short circuit, and significantly reducing the cycle life of AZMBs. Furthermore, metal zinc is prone to the hydrogen evolution reaction (HER) in aqueous electrolytes.[198] The HER competes with zinc deposition, affecting the normal progress of the electrode reaction and causing battery swelling. As the HER reaction continuously consumes H^+, local pH changes lead to the formation of electrochemically inert by-products.[199] Subsequently, these by-products passivate the zinc/electrolyte interface, reducing the cycling coulombic efficiency of AZMBs.

The methods for the modification of zinc anodes are mainly achieved from two perspectives, *i.e.*, optimizing the bulk structure and surface treatment. Zinc alloying is an important method for optimizing the bulk structure, and the metals currently used for alloys mainly include Ni,[58] Cu,[200–202] In,[203] Al,[204,205] Ag,[206] Ti,[207] and Bi.[208] This method has potential to inhibit dendritic growth, HER, and surface corrosion. The formed alloys show a microstructure different from pure zinc, and the changes in these microstructures can slow down the diffusion of corrosive media and improve the corrosion resistance.[209] Also, the addition of alloying elements can suppress the occurrence of HER by affecting the hydrogen evolution overpotential and the ability of zinc to bind with protons.[210] Alloying also promotes the dense deposition of zinc, and the decrease in Gibbs free energy leads to mixed nucleation and growth modes, which contribute to the uniform distribution of zinc atomic nuclei in space.[211] However, the alloy anodes in AZMBs generally encounter challenges such as volume changes, active particle fracture, and reduced reversibility during the charge and discharge processes.[212] Another important method is surface modification using materials such as metal oxides,[213] carbon-based polymers,[214] molecular sieves,[215] and alloys.[216] Generally, the modified layer can regulate the transport path of zinc ions through its pore structure or chemical properties, optimize the electric field distribution at the electrolyte/anode, and suppress the dendrite growth of zinc during the charge and discharge processes.[215] The modified layer isolates the surface of the zinc anode from the electrolyte, reducing the reaction between zinc and the active water molecules in the electrolyte and minimizing the occurrence of side reactions. However, the modified layers may gradually fail during long-term use of the battery, and thus their long-term stability and durability need to be studied.[217] The application of HEMs in AZMB anodes can be achieved through two main methods, *i.e.*, high entropy surface engineering and high entropy materialization (Fig. 17).

High entropy surface engineering. HEMs can serve as ideal coating materials to enhance the performance of anode materials. (1) Enhance the stability of the modified layer. The combination of multiple elements greatly helps to strengthen the structural stability of materials. Due to the pinning effect of the O and TM bonds, as well as the high entropy strategy, which can regulate the basic physical properties of materials, the high entropy modified layer with good mechanical properties and structural stability can suppress the structural instability caused by the shuttle of the highly polar zinc ions during the charge and discharge processes, extend the service life of the interface functional protective layer, and further improve the service life of the anodes. (2) Accelerate ion transport. The unique charge distribution of HEMs can promote continuous high-speed ion transport. The multimetallic compositions of HEM lead to complex electronic structures, and the interaction of valence electrons among multiple elements may alter the local electron cloud density, thereby affecting the distribution of charges.[218] HEM can form continuous and uniformly distributed potential gaps on the surface and bulk structure, effectively generating a built-in electric field, promoting the redistribution of mobile charges, and establishing gradients in the built-in electric field.[219] This gradient enhances the point-to-point electron transfer and promotes continuous ion transport.[220]

In addition to using high-entropy compound materials as modification layers, introducing continuous HEAs as modification layers is also feasible. By forming a uniform interface with abundant zinc affinity sites and magnetism, it can promote the uniform nucleation and deposition of metallic zinc. The high mechanical strength and corrosion resistance of HEAs can provide physical and chemical stability and inhibit dendrite growth.[220]

The existing results emphasize the feasibility of introducing high entropy surface engineering into AZMBs.[135] As shown in

Fig. 14(a), the modification process involves constructing a self-supporting layer of ultrafine high-entropy nanoparticles (approximately 2 nm) on the surface of the zinc anode. These nanoparticles act as zinc-friendly sites and exhibit a continuous distribution of potential gaps and a built-in electric field, reducing the activation energy for multi-electron reactions and regulating ion transport during zinc deposition (Fig. 14(b)). The hydrophobic nature and effective desolvation capability of these ultrafine high-entropy nanomaterials prevent unfavorable side reactions at the zinc anode, thereby enhancing the zinc deposition process (Fig. 14(c)).

High entropy materialization. AZMBs are based on zinc metal as the anode, and anodic high entropy alloying shows potential in optimizing the anode stability. The atomic strain fields in HEAs exhibit a more randomized distribution, altering the statistical distribution of lattice strain and augmenting the resistance to dislocation slip, thereby enhancing the structural stability. The staged alloying characteristics between elemental components help to buffer the volume expansion during alloying/dealloying processes.

Currently, HEMs have not been directly utilized as anode materials in AZMBs, but the introduction of more metallic elements into alloys has been preliminary explored. For example, the ZnLiMn alloy regulates the electrodeposition process through the generation of Li^+ and Mn^{2+} ions, creating an electrostatic shield mechanism that restricts the lateral diffusion of Zn^{2+}.[221] The huge crystalline stresses induced by Zn deposition can lead to significant cracks on the Zn anode surface, which are associated with capacity loss and should be mitigated by appropriate methods.[151] Some effective strategies have been implemented to address stress issues and encourage uniform nucleation. These strategies include the introduction of metal solid solutions and the formation of stable chemical bonds.[222] Innovative research has shown that a liquid metal anode containing three types of elements (ZnGaIn) could successfully alleviate deposition stress and eliminate nucleation barriers. The stress can be released by creating surface wrinkles, which facilitate zinc plating.[217] Furthermore, spontaneous alloying between Zn and liquid Ga–In has demonstrated enhanced cycling stability. Although alloys with five and more metal element have not been introduced as anodes for AZMBs, preliminary attempts have been made, and positive results in other systems offer possibilities for their application.

The full capabilities of HEMs in AZMBs remains insufficiently explored. The journey towards unlocking the potential of HEMs as anode materials in AZMBs may depend on a comprehensive understanding of their intrinsic properties and how these properties can be aligned with the distinctive characteristics of zinc-ion electrochemistry.

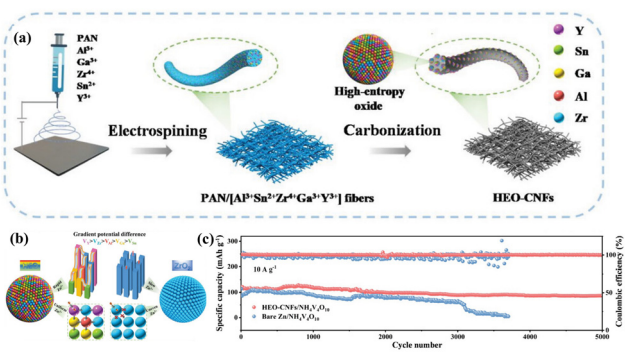

Fig. 14 (a) Process for the synthesis of HEO as anode of AZMB. (b) Mechanism of HEO for improving the electrochemical performance of zinc ion anode (c) long-term cycling performance of the anode modified with HEMs.[135]

5. HEMs as electrolytes with boosted ion transport kinetics

The key development directions of electrolytes include improving their ion conductivity, enhancing their stability, and optimizing the interface compatibility between the electrolyte and electrode materials. The rapidly developing energy storage industry has brought new challenges to the existing electrolytes. Energy storage devices need to meet the requirements of maintaining a good performance in extreme environments and supporting rapid charging and discharging, which puts higher demands on the low-temperature performance and ion conductivity of electrolytes. The introduction of the high-entropy concept in electrolytes is aimed at utilizing its various mechanisms of action to effectively improve their comprehensive performance such as low-temperature performance, ion conductivity, and electrochemical stability. This breakthrough will help expand the application fields of energy storage devices.

5.1 HEMs as electrolytes in other systems

The cycle performance of LIB and SIB deteriorates at low temperature, mainly due to the effect of the slow kinetics of the electrolyte. The viscosity of the electrolyte increases with a decrease in temperature, limiting the movement of ions and solvent molecules and slowing down the diffusion rate of ions. The slowed movement of ions leads to a decrease in the conductivity and increases the internal resistance of the battery. At the same time, low temperature conditions will increase the energy barrier required for ion desolvation, resulting in slower charge transfer reactions of ions at the electrode interface. The kinetic processes at the electrode–electrolyte interface, such as ion adsorption and insertion, will also slow down, affecting the charging and discharging efficiency of the battery.[223]

HE-electrolytes are still in the early stages of research. HE-electrolytes achieve high-entropy strategies by altering the specific composition or configuration in the solvation structure of metal cations. Firstly, HE-electrolyte helps to enhance the ion conductivity. (1) An increase in the configuration entropy induces local disorder, resulting in inhomogeneous interactions between different ions or molecules, allowing some ions to dissociate more readily and move freely, increasing the number of free-moving ions in the system, and thus enhancing the diffusion of ions and the overall ionic conductivity.[224]

(2) The increased entropy drives the thermodynamic equilibrium, making the metal cations more inclined to interact with the solvent molecules, inhibiting the formation of ion clusters and reducing the cluster volume (Fig. 15(a)).[225] This effect reduces ion aggregation, increases the free space for ion migration, and accelerates the ions migration process (Fig. 15(b)), thereby improving the ion conductivity of the electrolyte. (3) An increase in the number of components leads to a more diverse distribution of diffusion barriers for different solvation structures, which broadens the available percolation network and provides more low-energy ionic diffusion channels, effectively promoting the diffusion of charge carriers, and significantly improving the conductivity of the electrolyte (Fig. 15(f)).[225]

Secondly, HE-electrolytes can affect the deposition/stripping process of ions and the temperature range of electrolyte application. Changes in the composition of solvation groups alter the ion-solvent molecule interactions as well as the desolvation barriers of the metal ions, modulating the desolvation process of the charge carriers and the deposition/stripping process of the metal ions, achieving a denser and more uniform deposition morphology (Fig. 15(j)) and improving the overall electrochemical performance of the battery (Fig. 15(c)–(e)).[226] The complex solvation structure leads to stronger solvation effects by altering the interactions between the solute ions and solvent molecules. This effect increases the mixing enthalpy of various salts in HE-electrolytes and reduces the Gibbs free energy, thereby increasing the solubility of solutes and reducing the tendency for solute crystallization.[230] In addition, the entropy increase effect of HE-electrolytes disrupts the orderliness of the solid-state lattice, making the solid phase unstable, lowering the solid–liquid coexistence temperature, and resulting in a decrease in melting point, which helps to achieve a better low-temperature performance (Fig. 15(g)) and expands the actual temperature range of battery applications.[226]

The entropy control of the liquid electrolyte components has achieved high conductivity and optimized kinetic behavior in

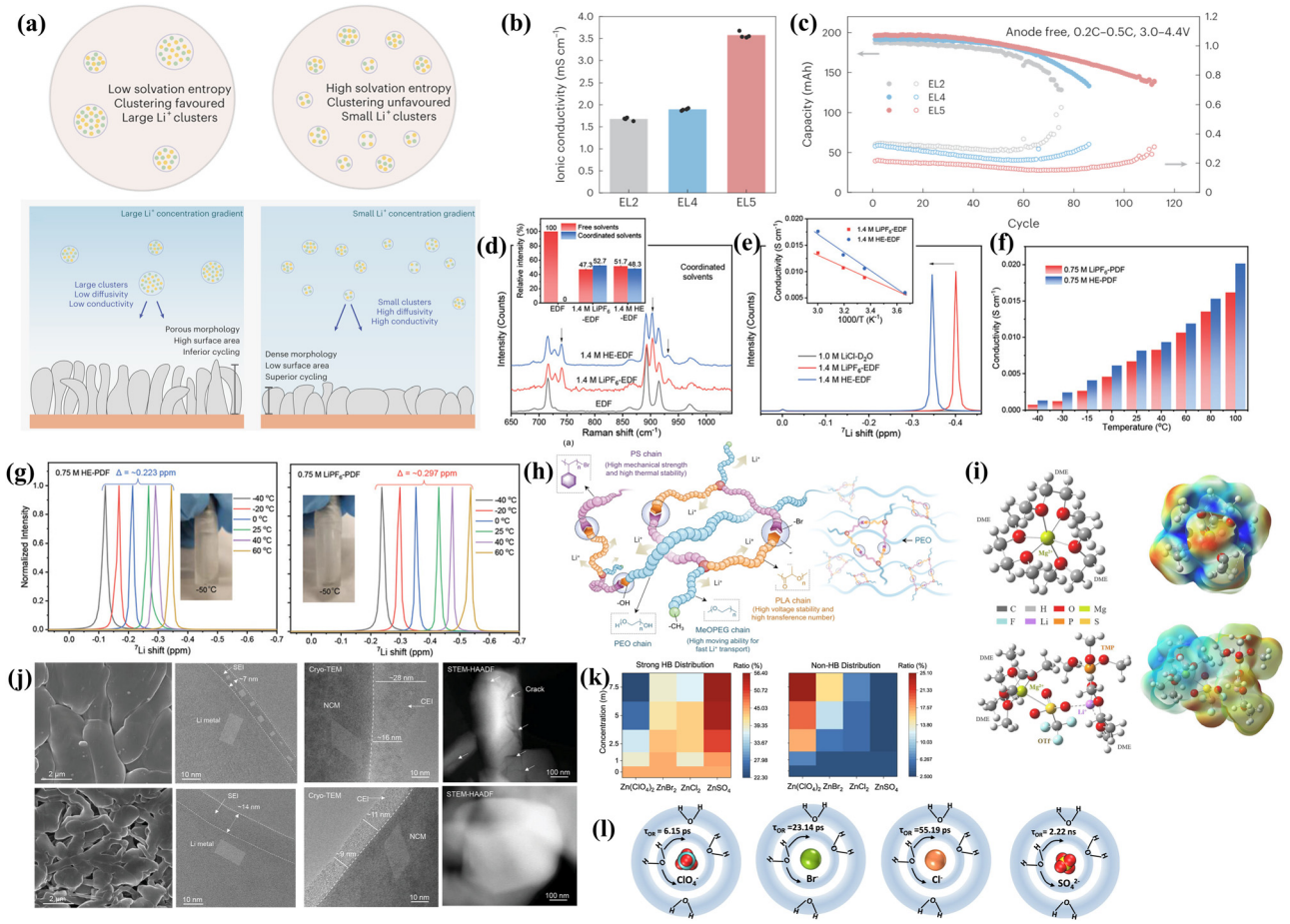

Fig. 15 (a) Illustration of solution structure in different electrolytes.[225] (b) Ionic conductivity of electrolytes of different components. (c) Electrochemical cycling performance of electrolytes with different components.[225] (d) Raman spectra of the 1.4 M HE-electrolyte and traditional electrolyte. (e) Liquid ^{7}Li NMR spectra of 1.4 M HE-electrolyte and traditional electrolyte. (f) Ionic conductivity of the 0.75 M HE-electrolyte and traditional electrolyte at various temperatures. (g) Variable temperature liquid ^{7}Li NMR spectra of 0.75 M traditional electrolyte and 0.75 M HE-electrolyte.[226] (h) Schematic of high-entropy microdomain interlocking polymer electrolytes.[227] (i) Typical solvation sheaths and corresponding electrostatic potential distribution of Mg $(TFSI)_2$/DME and Mg $(TFSI)_2$/DME with LiOTf/TMP electrolytes.[228] (j) Cryo-TEM images of anode and cathode in 1.4 M HE-electrolyte and 1.4 M traditional electrolyte.[229] (k) Proportion of water with strong (left) and non-HB (right) in four electrolytes at different concentrations fitted from Raman spectra. (l) Schematic of water structure around ClO_4^-, Br^-, Cl^- and SO_4^{2-}.[228]

the design of magnesium metal battery (MMB) electrolytes. By co-adding LiOTf and TMP salts to the $Mg(TFSI)_2$/DME-based electrolyte, an electrolyte with a high-entropy solvation structure of Mg^{2+}-2DME-OTf^--Li^+-DME-TMP was formed, as shown in Fig. 15(i).[229] The unique solvation structure effectively weakens the strong interaction between the Mg^{2+} ions and DME solvent, thereby reducing the solvation potential barrier of Mg^{2+}. This solvation structure brings OTf^- and TMP to the surface of the Mg anode, promoting the formation of an $Mg_3(PO_4)_2$-rich layer, preventing the formation of insulating components on the anode surface, and facilitating an improvement in the conductivity of Mg^{2+}.

Solid-state electrolytes offer higher safety; however, they face the complex challenges of simultaneously improving their mechanical strength and accelerating ion migration. HE solid electrolytes exhibit excellent performances in terms of ion transport kinetics, cycling performance, mechanical properties, and other aspects. HE-electrolytes introduce chemical disorder, resulting in a more uniform distribution of site energy, which helps break the long-range order of atomic arrangement in traditional solid-state electrolytes and may simultaneously improve the ion transport kinetics and cycle performance.[231] Moreover, the introduction of the high-entropy concept into solid electrolytes leads to local structural distortions, and the overall energy state of solid electrolytes is more dispersed, which helps to reduce the energy barrier for ion migration in the materials, and thus improve the ion conductivity.[232] Solid electrolytes with increased configurational entropy not only possess excellent mechanical strength, but also maintain high ionic conductivity and stable Li^+ migration numbers in complex and dynamic environments, thereby improving the reliability and durability of their overall performance.[227] By combining strategies such as entropy elasticity, supramolecular self-assembly, and topological chemical polymerization, polymer electrolytes with high-entropy microdomain structures with increased configuration entropy can be effectively designed (Fig. 15(h)), which simultaneously improves the mechanical strength and ionic mobility of the materials, and endows them with excellent multifunctionality and environmental adaptability.[228]

5.2 Expected implementation of HEM electrolytes in AZMBs

Aqueous electrolytes have received widespread attention due to their inherent safety, excellent ion conductivity, and significant environmental friendliness. However, the practical application of aqueous electrolytes faces significant challenges. Based on the classical Pourbaix plot, which illustrates the relationship between electrolyte pH and HER/OER potentials, the operating voltage range of AZMBs is limited to a relatively narrow ESPW of approximately 1.23 V.[233] The limited electrochemical window of the electrolyte restricts the operating voltage and energy density of AZMBs. Meanwhile, the low boiling point and high freezing point of water, as well as the intensified side reactions within the battery at high temperatures, greatly limit the widespread application of AZMBs.[234] In addition, the deposition process of metal ions is not only closely related to the properties of the metal anode, but also significantly affected by the way they act in the solvation group.[235] Therefore, it is crucial to modulate the solvation structure to optimize the deposition behavior of metal ions to achieve higher interfacial stability.

Currently, the common methods to expand the ESPW of electrolytes and broaden the temperature range for their application include adjusting the solute concentration in the electrolyte,[236] introducing different soluble salts,[237] and adding organic additives.[238] HE-electrolytes can significantly optimize the kinetic performance, enhance the zinc ion conductivity under low temperature conditions, and effectively suppress side reactions on the surface of the zinc anode, thereby enhancing the overall performance of aqueous zinc ion batteries.

The introduction of the high-entropy strategy can significantly optimize the kinetic properties of the electrolyte. The inherent hydrogen bonding network in aqueous electrolytes can affect the viscosity and conductivity of the electrolyte. Strong hydrogen bonding networks can limit the movement of ions, and an increase in the entropy of the electrolyte can disrupt the continuous hydrogen bonding network between water molecules.[225] By disrupting the hydrogen bonding network, the viscosity of the system can be reduced, thereby improving the migration speed of the solvation groups. Meanwhile, the high-entropy strategy can affect the interaction between the metal ions and solvent molecules, which in turn affects the desolvation process and ion dissociation behavior, and this effect can significantly increase the overall ion mobility of the electrolyte, thus improving the kinetic properties.[239]

HE-electrolytes can break the inherent solubility limitation of soluble salts and enhance the kinetic performance of AZMBs operating at low temperatures. By modulating the diversity of soluble salts and solvent molecules in the electrolyte or designing electrolytes with higher configurational entropy, the increase in entropy increases the degrees of freedom of the electrolyte and significantly enhances the solubility.[224] Firstly, an increase in the configurational entropy directly affects the distribution of soluble salts and solvent molecules in the electrolyte, which makes it easier to be dissolved; secondly, the multi-component high-entropy effect of dissolved salts and solvents can produce eutectic effects, reducing the melting points of the components and further increasing their solubility at room temperature.[240] An increase in configurational entropy can also affect the freezing point of the electrolyte, and this chaos and disorder increases the free energy of the system, thereby reducing the tendency of the system to form an ordered solid state (*i.e.*, solidification).[241] It also helps maintain good ion transport kinetics at low temperatures.

The formation of high-entropy aqueous electrolytes can effectively suppress the side reactions occurring on the surface of metal anodes. HE-electrolytes regulate the solvation structure of Zn^{2+} by introducing multiple components or utilizing various configurations of Zn^{2+} with anionic/solvent molecules.[232] This regulation can optimize the solvation environment of ions and reduce the amount of active water molecules in the solvation groups. The reduction of reactive water molecules contributes to the disruption of the hydrogen bonding network between water molecules, which in turn weakens the reactivity of water. Under the action of an electric field, these optimized solvation groups

can be enriched in the double-layer structure at the electrolyte/electrode interface, which effectively avoids side reactions such as HER and corrosion occurring on the surface of the zinc anode.

The synergistic effect of HE-electrolytes can achieve a combination of multiple advantageous characteristics, which further enhances their comprehensive performance. For example, by introducing solvent molecules with weak solvation properties to replace some water molecules, the desolvation barrier of Zn^{2+} can be significantly reduced, which can accelerate the deposition kinetics of Zn^{2+} and enhance the coulombic efficiency of the zinc anode. Meanwhile, other components within the same solvation structure, such as certain anions and organic molecules, may play a crucial role in promoting the formation of a solid electrolyte interface (SEI) film, which helps to balance the ion concentration and charge density on the surface of the zinc anode, and thus promotes the uniform deposition of Zn^{2+}. In addition, by regulating the electron density distribution and Fermi energy level of these components on the surface of the zinc anode, the proton adsorption characteristics of the surface are affected, thereby increasing the overpotential for HER. By inhibiting the electrochemical decomposition behavior of water, and thus broadening the electrochemical window of the electrolyte, the energy density of the batteries its improved. These performance enhancements are due to the synergistic effect of the multiple components in the HE-electrolyte, and thus it is difficult for traditional additives to achieve this comprehensive functional optimization.

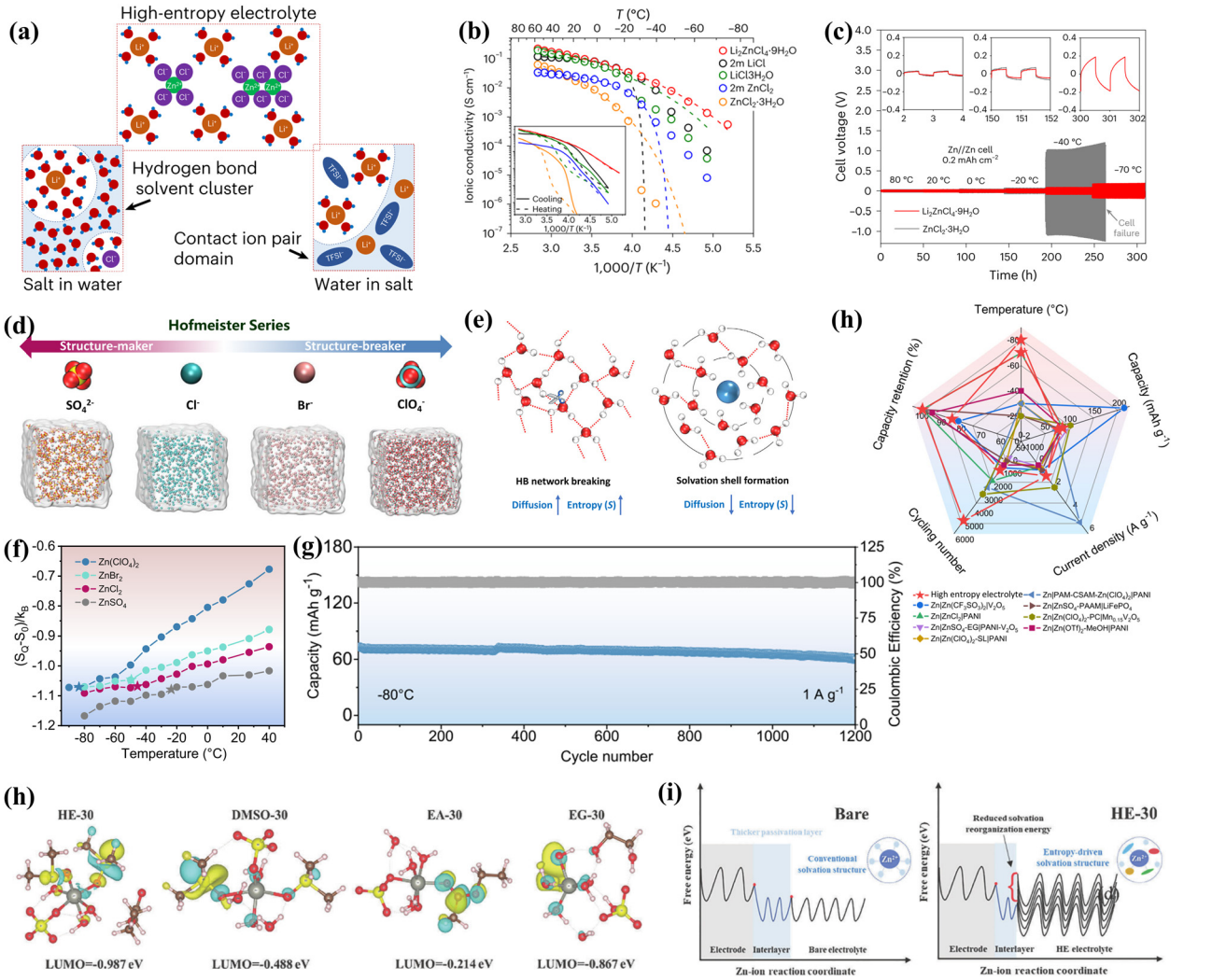

Fig. 16 (a) Schematic of the solution structure in an HE-electrolyte and traditional electrolyte. (b) Arrhenius plots of the overall ionic conductivity of $Li_2ZnCl_4{\cdot}9H_2O$ electrolyte compared with concentrated $LiCl{\cdot}3H_2O$, $ZnCl_2{\cdot}3H_2O$ solutions and dilute LiCl and $ZnCl_2$ aqueous solutions. (c) Galvanostatic Zn stripping/plating in a Zn||Zn symmetrical cell with $Li_2ZnCl_4{\cdot}9H_2O$ and $ZnCl_2$ electrolyte at 0.2 mA cm^{-2} and temperature range of +80 °C to −70 °C.[225] (d) Hofmeister series with four diverse anions and the models of the corresponding four aqueous zinc salt solution for MD simulations. (e) Original water molecules form a tetrahedral network structure through hydrogen bonding. (f) Comparison of the performances of AZMBs with HE-electrolyte and the former electrolytes at low temperatures. (g) Tetrahedral entropy of water molecules in HE-electrolytes over the temperature range of −80 °C to 40 °C. (h) Cycling performance of AZMBs based on HE-electrolyte at −80 °C.[228] (i) LUMO energy levels of Zn^{2+} clusters in four types of electrolytes. (j) Schematic of Zn ion transport between electrodes and electrolytes in HE-electrolyte and conventional electrolyte.[228]

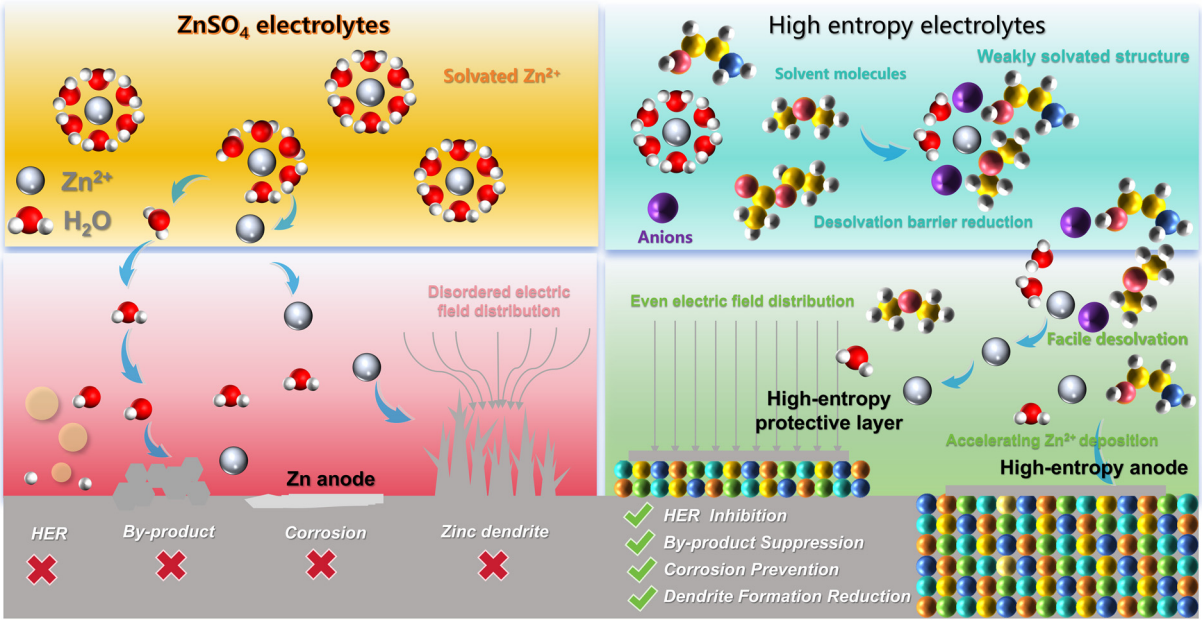

Fig. 17 Schematic of the introduction of high-entropy anode and high-entropy electrolyte to solve the problems occurring at the anode in AZMBs.

Preliminary progress has been made in the application of HE-electrolytes in AZMBs, which not only broadens their electrochemical stability window and the operating temperature range, but also suppresses the interfacial side reactions, achieving an improvement in the coulombic efficiency of Zn^{2+} deposition/stripping. The introduction of the support salt LiCl into the $ZnCl_2$ electrolyte, utilizing Zn^{2+} and Cl^- to form anion clusters $[ZnCl_{4-m}^{2-m}]_n$ with different lengths and structures, resulted in a high-entropy solvation structure (Fig. 16(a)).[225] Based on this electrolyte system, the preferential coordination of free water with Li^+ at low salt concentrations and the elimination of free water at high salt concentrations reduced the content of reactive water molecules in the solvation clusters and disrupted the hydrogen-bonding network in the solvent water, optimizing the reversibility of the Zn deposition/stripping. The length of the anion clusters is limited by the decrease in water molecules and the increase in Li–Cl contact, thus maintaining high ionic conductivity (Fig. 16(c)). The significant decrease in solvent activity suppresses the shrinkage and crystallization of the solvent clusters at low temperatures, thereby expanding the temperature range suitable for electrolytes. In addition, there is a direct correlation between the entropy value of the tetrahedral network structure formed by water molecules through hydrogen bonding and the freezing behavior of water in the Zn^{2+}-based electrolyte (Fig. 16(g)).[228] Different anions were utilized to alter the configuration entropy of the tetrahedral network structure formed by hydrogen bonding of the original water molecules (Fig. 15(l) and 16(d)), and the relatively weak interactions between the "structure-breaking" ClO_4^- anion and water molecules promotes their migration, resulting in a more disordered distribution of water molecules and endowing them with the highest tetrahedral entropy, which helps to achieve optimal frost resistance, while the introduction of SO_4^{2-} gives water the lowest tetrahedral entropy, providing the worst frost resistance, as shown in Fig. 16(e). The AZMBs based on the electrolyte with the highest tetrahedral entropy successfully operated at −80 °C and achieved a capacity retention rate of approximately 85% after 1200 cycles (Fig. 16(f) and (h)). The introduction of the high-entropy strategy also helps to enhance the cyclic reversibility of Zn deposition/stripping. By mixing volumes of ethyl acetate (EA), ethylene glycol (EG), and dimethyl sulfoxide (DMSO) as solvent components to increase the entropy of the electrolyte system, this strategy not only changes the solvation sheath composition and structure of Zn ions in the electrolyte environment, but also induces the hydrogen bonding reconstruction of the water molecules in the solvent due to the complex solvent composition.[239] As shown in Fig. 16(i), Zn clusters exhibit different LOMO energy levels in different solvents. The lowest LUMO of HE-30 indicates that this electrolyte has a strong electron affinity and tends to decompose and form a passivated intermediate layer. In addition to its key role in mitigating surface corrosion, the synergistic coupling of mixed co-solvents effectively utilizes the characteristics of individual solvent additives and promotes significant advantages in cycle reversibility (Fig. 16(j)).

The utilization of electrolyte additives to regulate the electrode double layer (EDL) structure of the zinc anode is an effective strategy for suppressing interface side reactions and promoting uniform zinc deposition. The design of an EDL with multi-component collaborative functionality was inspired by the concept of high entropy.[242] The addition of diphenylsulfonylimide (BBI) and $LaCl_3$ additives to $ZnSO_4$ electrolyte achieved the high-entropy strategy by regulating the number of components in EDL. EDL contains high-valence cations, anions, anions forming an SEI layer and the zinc ion solvation

groups in the desolvation process. Different components in high-entropy EDL have different functions, where La^{3+} preferentially adsorbs and aggregates at the dendrite tip, shielding the concentration electric field and allowing the Zn deposition layer to grow uniformly. Meanwhile, a net depletion zone is formed near the Zn surface, attracting more BBI anions or Cl^- ions into EDL. As Zn deposition proceeds, the Cl^- ions promote the desolvation process of the Zn^{2+} ions within the EDL and accelerate the kinetics of Zn deposition. The BBI anions are reduced to generate BBI-derived components, forming a strong SEI layer with high mechanical strength, which enhances its ability to inhibit corrosion reactions and dendrite formation.

In summary, the inherent structure and chemical diversity of HE-electrolytes are considered to be a strong candidate for addressing the complex challenges faced by the aqueous electrolytes of AZMB. Currently, the application of HE-electrolytes in AZMBs has shown initial results, and the synergistic effect of multiple components has achieved a better comprehensive performance based on single-component additives. HE-electrolytes can not only reduce the solvation energy barrier of Zn^{2+}, improve the coulombic efficiency of Zn^{2+} deposition/stripping, and effectively suppress interfacial side reactions, but also broaden the operating temperature range. These advances have laid a solid foundation for the further development of AZMBs. In the future, by providing microscopic control and optimization within the electrolyte system, we can further enhance the performance and promote the widespread application of high-performance and long-life AZMBs.

6. Summary and outlook

In this perspective, based on the existing application of HEMs in the field of secondary energy storage, we analyzed and assessed the potential and effective application paths of HEMs in AZMBs. The application of HEMs in AZMBs has made initial progress, especially in solving the existing problems of interface side reactions at the anode as well as insufficient kinetic and low-temperature performances of the electrolyte, demonstrating great potential. In the future, it is expected that HEMs will continue to develop with superior performances through further material optimization and design to promote the practical application and commercialization process of AZMBs. Firstly, herein, we focused on the specific application methods and reaction mechanisms of HEMs in LIBs and SIBs. Based on the similarity between AZMBs and these two systems in terms of battery structure, electrode materials and failure mechanisms, initially the three key components, namely, cathode, anode and electrolyte, were introduced and the specific problems that HEMs may solve in AZMBs explored in detail, looking forward to its application in this field.

The practical application of AZMBs is hampered by the failure behavior of various important battery components, including structural degradation of the commonly used cathodes, dendrite growth/side reactions on the surface of the zinc anode, and the narrow electrochemical windows and temperature ranges of aqueous electrolytes. In terms of the cathode, cathode materials based on the high-entropy effect, lattice distortion, pinning effect, and cocktail effect exhibit characteristics such as enhanced structural stability, prolonged cycle life, widened operating voltage, delayed phase transition, and accelerated transmission kinetics, which are expected to solve the common problems of poor structural stability, phase transition, and slow kinetics in cathodes in AZMBs. In terms of the anode, high entropy surface engineering and high entropy materialization endow materials with high structural stability. The optimized electrolyte/electrode interfaces are conducive to a uniform surface metal ion and electric field distribution, achieving uniform ion deposition and rapid kinetics. When applied in AZMBs, different surface/bulk components may increase the overpotential of HER and inhibit the occurrence of side reactions, while achieving a uniform deposition with homogeneous electric field distribution. In terms of electrolyte, the complex salt/solvent compositions are conducive to enhancing the configuration entropy of metal ions in the electrolyte. The change in configuration entropy significantly affects the viscosity and temperature range of the electrolyte. The solvation structure of metal ions in HE-electrolytes can be adjusted to reduce the number of free water molecules in the EDL and disrupt the hydrogen-bonding network of the water molecules in the original electrolyte. The introduction of high-entropy components or high-entropy configuration changes the composition and solvation effect of metal anions/solvents in the solvation structure, which in turn solves the side reactions such as HER and corrosion in AZMBs, broadens their application temperature, and realizes the rapid desolvation and uniform deposition of Zn^{2+}. Besides, we provided a detailed description of the definition, mechanism of action, and methods for the synthesis of high entropy, which guides the direction in selection and synthesis. Although the application of HEM is still in its infancy, it can be predicted that this strategy has great potential in alleviating the shortcomings of existing AZMBs.

In addition to the specific descriptions provided in each subsection, we also offer insights into potential future research directions. These insights are intended to guide the integration of HEMs in AZMBs to achieve efficient energy storage. Fig. 18 shows a schematic diagram of these implementation paths.

Theoretical calculations should be employed to screen suitable HEMs

HEMs have demonstrated unprecedented properties, but their exploration and development present significant challenges. Due to their complex atomic arrangement and element interactions, which are difficult to determine, it is necessary to carefully decouple the actual effects of the individual elements on the intrinsic properties and electrochemical behaviors. Currently, no database has been established to directly exhibit the relationship between the elemental composition and stoichiometry in HEMs and their fundamental properties. To pinpoint the desired characteristics, a large number of controlled experiments is necessary to determine the optimal types and ratios of various elements.

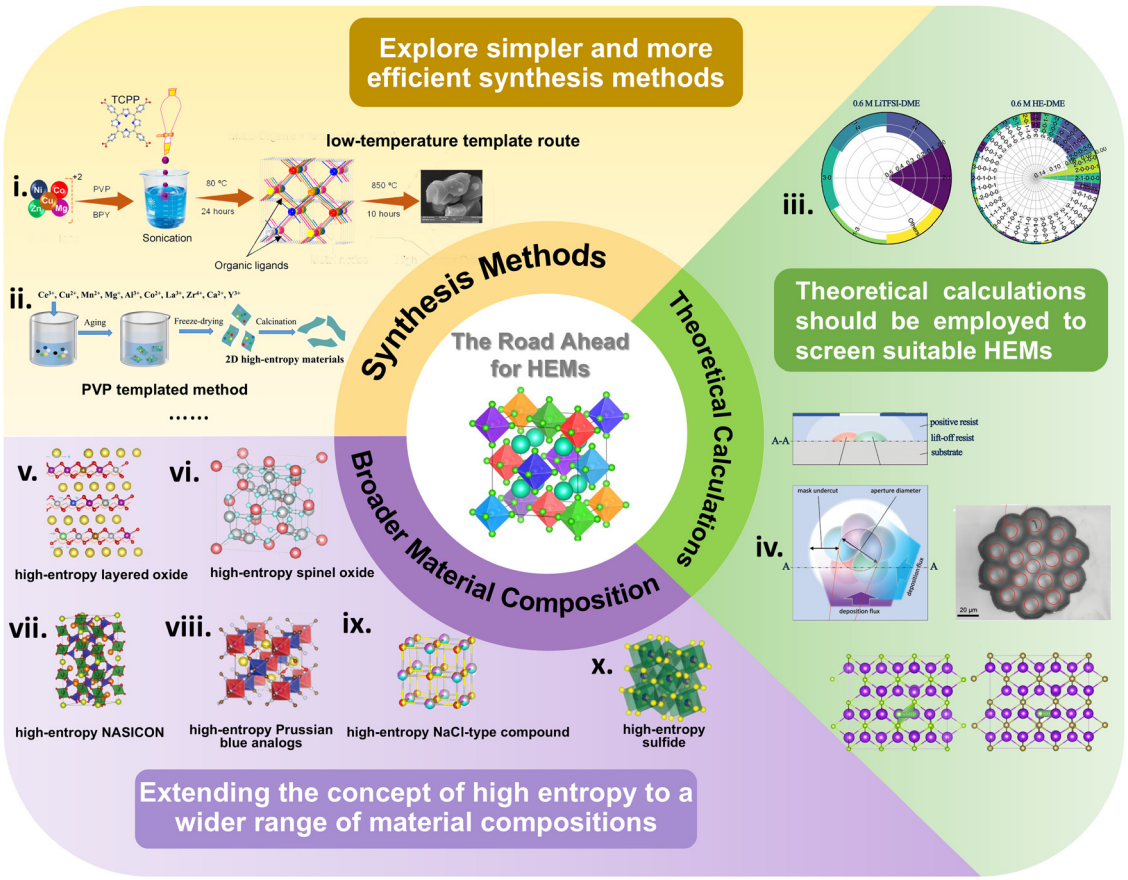

Fig. 18 Road ahead for HEMs.[60,243–251]

Expand the concept of high entropy to broader material composition

Nowadays, there are significant limitations in the application of high-entropy concepts. When studying the concept of high entropy, most of the research tends to be limited to the study of high-entropy components, ignoring the deeper role of configuration. The majority of HEMs investigated are based on the multiple species of cation ion doping, achieving improvements in stability, specific capacity, and kinetic performance. Inspired by the configuration entropy in HE-electrolytes, it is possible to introduce defects or substitute anions in the development of electrodes to introduce configuration entropy, thereby affecting the performance of materials.

Explore simpler and more efficient synthesis methods

It is urgently needed to delve deeper into the development of efficient, large-scale preparation methods for HEMs that facilitate facile synthesis, mild reaction conditions and cost-effectiveness. This approach is crucial for facilitating the transition of HEMs from laboratory research to practical and industrial-scale production. The realization of HEMs requires consideration of the temperature conditions and reaction environments under which the introduced metal ions or anions enter the lattice interior of the materials, as well as the balancing of the negative effects of structural collapse and defect diffusion generated during the synthesis process on the material properties.

HEMs require careful assessment of their cost and environmental impact. Solid-state electrode materials are often based on high-entropy compositions, typically consisting of compounds with multiple metal ions. Thus, to leverage the cocktail effect of HEMs for the comprehensive optimization of material properties, it is common to introduce metal ions with different electronic properties or chemical states. The uniqueness of HEMs lies in their complex lattice structures formed by the random arrangement of multiple metals, but these complex structures also pose challenges for electron conduction. To improve the electrical conductivity and reaction kinetics, existing research introduced transition metals with d-bands, such as Ni, Co, and V. The interaction of d-orbital electrons among different metal atoms in HEMs can enhance electron migration. The overlapping of d-bands from various transition metal ions helps form continuous conductive pathways, allowing more electrons to participate in the conduction process, and thereby increasing the electrical conductivity. To enhance the capacity of HEMs, researchers consider incorporating high-valence metal ions, which can achieve more electron transfer through multiple valence redox reactions during battery cycling, leading to higher energy density, such as Co, Ni, Ti,

V, and Ta. Despite playing a key role in enhancing the battery performance and remaining in laboratory research with relatively small amounts of additives, the high cost and limited supply of these metals pose challenges for large-scale commercial application. These expensive rare or noble metals not only increase the production cost of materials but also place higher demands on the stability of the supply chain. Thus, by substituting rare metals with cheaper elements with stable supply chains, the cost of materials can be reduced. For example, using relatively inexpensive elements such as Fe and Mn as components of high-entropy materials can significantly reduce costs, but there may still be performance issues that do not meet expectations in specific applications. Moreover, due to their unique mechanism, HEMs require precise control of the ratio of added metal elements to achieve expected and stable material performance, but the performance of HEMs often depends on the high purity of the elements, and the extraction and processing of high-purity elements involve high costs, which can significantly increase the costs in large-scale production. Furthermore, to ensure the stability and consistency of synthesized materials and avoid side reactions due to the introduction of multiple elements under different synthesis conditions, issues such as uncontrollable phase separation, element volatilization, and different reaction rates need to be strictly controlled in the synthesis process, which requires expensive equipment and precise control. Processes commonly used in laboratories, such as high-temperature melting, vacuum furnaces, and mechanical alloying, work well for small-scale production, but the cost and equipment requirements of these processes may be beyond the feasible range for large-scale production.

In the case of liquid high-entropy electrolytes based on high entropy components, the solubility and concentration of individual components and the compatibility between different components need to be considered. The solubility of high-entropy electrolytes not only affects their performance in batteries but also has a direct impact on the synthesis difficulty and cost of the overall material. Some components are difficult to dissolve within the operating temperature range and require special synthesis conditions, such as high temperature, high pressure, and the use of special solvents, which will increase the preparation cost of the material. The solubility of the components in HE-electrolyte systems may interfere with each other, and there may be poor compatibility, making the components unable to coexist in the solution, and leading to their precipitation or sedimentation, which affects the uniformity of the overall electrolyte. In addition, the electrolyte salts in AZIBs are usually high-purity salts, and the cost of high-purity salts is high. Introducing multi-component electrolyte salts will significantly increase the total cost of the electrolyte. Thus, to reduce the manufacturing cost of HE-electrolytes, it is necessary to fully analyze the compatibility between components before their preparation, which can avoid reactions or decomposition of certain components, avoid electrolyte failure and unnecessary phase separation or solid phase formation, thereby reducing additional material processing costs. By predicting the coexistence behavior of different components based on existing experimental data and selecting components with similar electrochemical properties to enhance the compatibility of the system, costs can be reduced.

HEMs exhibit many obvious advantages, including improving the stability and cycle life of the active substance in the case of the cathode, inhibiting dendrite growth and improving the Zn^{2+} deposition/stripping behavior at the zinc electrode, and enhancing the ion conductivity and broadening the electrochemical window in the electrolyte. However, HEMs are a double-edged sword and may bring some problems when applied in AZMBs, which need to attract sufficient attention and further research (Fig. 19).

Balancing energy density and cycle life

The introduction of electrochemically inert components in HEMs can help stabilize the complex material structure and improve the long-term stability of the materials. However, the introduction of inactive elements into HEMs can inevitably affect the energy density of the battery. Consequently, a delicate balance must be struck, carefully weighing the benefits of extended cycle life against the suitability for specific applications. Achieving this balance is crucial to ensure that the integration of HEMs enhances, rather than diminishes the overall performance and effectiveness of the battery system.

Defect engineering

The precise adjustment of point defect concentrations after introducing the high-entropy strategy is beneficial to enhance the conductivity of materials. However, the incorporation of metal ions into the lattice introduces various defects, which require careful evaluation. This challenge encompasses potential issues across various aspects, such as reducing the component heterogeneity, rectifying microstructural distortions, optimizing point defects, fine-tuning the electronic structure, and regulating ion migration. Moreover, dislocations within the material structure can trigger phase transitions, which may reduce the overall capacity of the battery. These dislocations also contribute to the formation of undesirable cracks, increasing the resistance and further degrading the electrochemical performance.

Interlayer spacing

An adequate interlayer spacing is instrumental for the intercalation of Zn^{2+} and protons in HEM cathodes. The introduction of ions with diverse volume sizes and charge numbers following the high-entropy transformation of materials can significantly influence the bulk structure. The interactions among various ions within the lattice may induce lattice distortion, causing the constituent atoms to deviate from their ideal positions. This deviation can potentially impact the channels available for ion intercalation. Considering the slow kinetics associated with polarized Zn^{2+} groups, HEMs that incorporate a variety of metal elements in their lattices must satisfy stringent requirements regarding interlayer spacing. This spacing is not only conducive to Zn^{2+} insertion/extraction

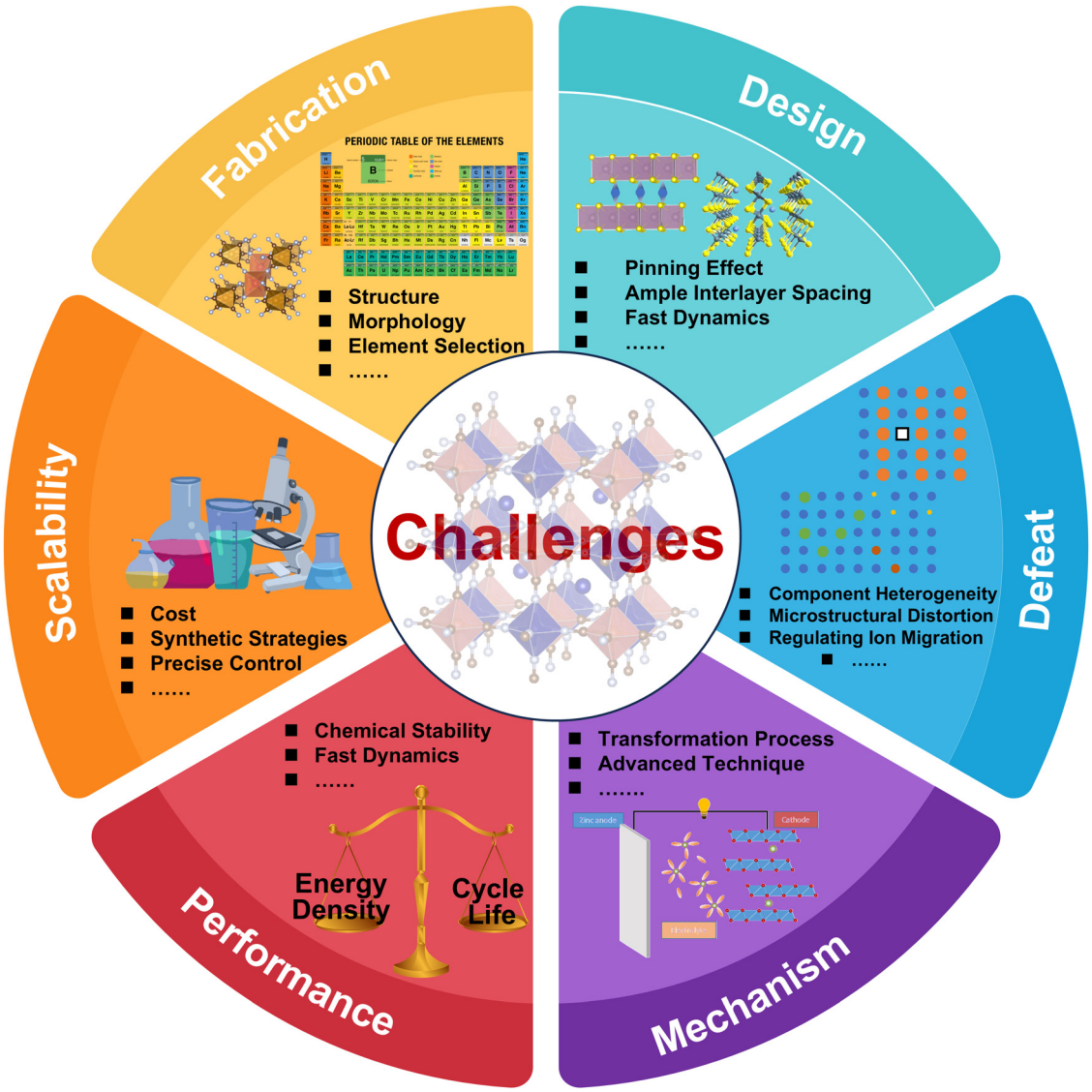

Fig. 19 Challenges that need to be considered in the development of HEMs in AZMBs.

but also significantly enhances the ion transport process and mitigates the electrostatic interaction between Zn^{2+} and the HEM substrates.

HEM anode reconsideration

HEMs as anodes hold significant potential for precisely controlling the zinc nucleation behavior and hydrogen evolution overpotential. However, there are critical issues that require careful reconsideration before their practical application. The complex strategies for the synthesis of HEMs pose significant cost challenges, especially for large-scale energy storage applications. Furthermore, HEMs are typically in powder form, and when used directly as anodes, their high specific surface area and the presence of hydrogen precipitation sites may trigger severe side reactions without further modification. The multiple metals in HEMs may interact with the electroplating process of zinc, thereby affecting the deposition behavior of Zn^{2+}. Under deep discharge conditions, the growth of zinc dendrites may become more pronounced, especially when the electroplating behavior of certain metals in HEMs is not coordinated with zinc. The competitive deposition behavior between different metal ions in HEMs may lead to a decline in the quality of zinc deposition, thereby affecting the discharge depth of the battery.

Electrolyte kinetics

Electrolytes containing HEMs have the potential to alter the chemical environment of water molecules, which can modulate the solvated Zn^{2+} ions and attenuate the electrostatic coupling between anions and cations. These effects can help inhibit corrosion, HER, and the generation of by-products. Nevertheless, it is critical to note that strong interactions between Zn^{2+} ions and the solvent molecules, driven by the high-entropy mechanism, may lead to challenging desolvation processes.

This can result in sluggish transfer kinetics for Zn^{2+} ions, ultimately leading to inhomogeneous deposition and dendrite formation. When strong solvation shells are formed, it becomes difficult for Zn^{2+} ions to intercalate into the cathode material or deposit at the anode surface. Therefore, the binding strength between the cation and the solvent must be carefully considered to optimize the performance of the electrolyte.

Synthesis process control

HEMs used as electrodes or solid-state electrolytes typically contain multiple metal ions, which may not be uniformly distributed within the lattice. When the sintering temperature is inappropriate or the reaction time is too short, phase separation may occur among the various metal components, resulting in uneven electrochemical reactivity of the material. Furthermore, during the charge and discharge cycles, the differences in the chemical properties and ionic radii of the metals may cause them to migrate and redistribute within the material, or even form independent phases. This process may be induced by the stress generated when zinc ions are inserted into and extracted from the electrode material, especially during deep discharge, where stress changes are more pronounced. Due to the differences in the chemical properties and lattice energy of the metal ions, some metals may precipitate from the original high-entropy structure during long-term cycling or deep discharge, forming localized oxides or other phases, which may negatively affect the overall electrochemical performance of the electrode material.

In conclusion, this perspective exhibited the potential and effective application path of HEMs in AZMBs. Although the application of HEMs is still in its infancy, it can be predicted that this strategy has great potential to alleviate the defects of the existing AZMBs. Meanwhile, the concerns regarding the compatibility of HEMs also need to be considered. It is vital to get a deep and thorough understanding of the fundamental chemistry of HEMs within the context of AZMBs. Future efforts should focus relentlessly on identifying the key elements and species that comprise HEMs, characterizing them with advanced testing methods and selecting the most suitable application scenarios.

Data availability

No primary research results, software or code have been included and no new data were generated or analysed as part of this review.

Conflicts of interest

There are no conflicts to declare.

Acknowledgements

This work was supported by the National Natural Science Foundation of China (Grant No. 22209013), and the BIT Research and Innovation Promoting Project (Grant No. 2024YCXZ025).

References

1 J. Xu, J. Zhang, T. P. Pollard, Q. Li, S. Tan, S. Hou, H. Wan, F. Chen, H. He, E. Hu, K. Xu, X.-Q. Yang, O. Borodin and C. Wang, *Nature*, 2023, **614**, 694–700.
2 X. Han, Y. Bai, R. Zhao, Y. Li, F. Wu and C. Wu, *Prog. Mater. Sci.*, 2022, **128**, 100960.
3 M. Lv, R. Zhao, Z. Hu, J. Yang, X. Han, Y. Wang, C. Wu and Y. Bai, *Energy Environ. Sci.*, 2024, **17**, 4871–4906.
4 R. Zhao, J. Yang, X. Han, Y. Wang, Q. Ni, Z. Hu, C. Wu and Y. Bai, *Adv. Energy Mater.*, 2023, **13**, 2203542.
5 B. Tang, L. Shan, S. Liang and J. Zhou, *Energy Environ. Sci.*, 2019, **12**, 3288–3304.
6 Y. Wang, X. Wang, A. Zhang, X. Han, J. Yang, W. Chen, R. Zhao, C. Wu and Y. Bai, *Small*, 2024, 2403136.
7 N. Zhang, X. Chen, M. Yu, Z. Niu, F. Cheng and J. Chen, *Chem. Soc. Rev.*, 2020, **49**, 4203–4219.
8 B. D. Boruah, A. Mathieson, B. Wen, S. Feldmann, W. M. Dose and M. De Volder, *Energy Environ. Sci.*, 2020, **13**, 2414–2421.
9 S. Wang, Z. Huang, J. Zhu, Y. Wang, D. Li, Z. Wei, H. Hong, D. Zhang, Q. Xiong, S. Li, Z. Chen, N. Li and C. Zhi, *Adv. Mater.*, 2024, **36**, 2406451.
10 R. Yao, Y. Zhao, L. Wang, C. Xiao, F. Kang, C. Zhi and C. Yang, *Energy Environ. Sci.*, 2024, **17**, 3112–3122.
11 D. Zhao, S. Chen, Y. Lai, M. Ding, Y. Cao and Z. Chen, *Nano Energy*, 2022, **100**, 107520.
12 X. Chen, H. Zhang, J.-H. Liu, Y. Gao, X. Cao, C. Zhan, Y. Wang, S. Wang, S. L. Chou, S. X. Dou and D. Cao, *Energy Storage Mater.*, 2022, **50**, 21–46.
13 F. Tang, X. Wu, Y. Shen, Y. Xiang, X. Wu, L. Xiong and X. Wu, *Energy Storage Mater.*, 2022, **52**, 180–188.
14 N. Zhang, J. C. Wang, Y. F. Guo, P. F. Wang, Y. R. Zhu and T. F. Yi, *Coord. Chem. Rev.*, 2023, **479**, 215009.
15 Y. Dai, C. Zhang, J. Li, X. Gao, P. Hu, C. Ye, H. He, J. Zhu, W. Zhang, R. Chen, W. Zong, F. Guo, I. P. Parkin, D. J. L. Brett, P. R. Shearing, L. Mai and G. He, *Adv. Mater.*, 2024, **36**, e2310645.
16 C. Liu, X. Xie, B. Lu, J. Zhou and S. Liang, *ACS Energy Lett.*, 2021, **6**, 1015–1033.
17 Z. Ye, Z. Cao, M. O. Lam Chee, P. Dong, P. M. Ajayan, J. Shen and M. Ye, *Energy Storage Mater.*, 2020, **32**, 290–305.
18 J. Wang, Y. Huang, B. Liu, Z. Li, J. Zhang, G. Yang, P. Hiralal, S. Jin and H. Zhou, *Energy Storage Mater.*, 2021, **41**, 599–605.
19 X. Lin, G. Zhou, J. Liu, M. J. Robson, J. Yu, Y. Wang, Z. Zhang, S. C. T. Kwok and F. Ciucci, *Adv. Funct. Mater.*, 2021, **31**, 2105717.
20 J. Yang, R. Zhao, Y. Wang, Z. Hu, Y. Wang, A. Zhang, C. Wu and Y. Bai, *Adv. Funct. Mater.*, 2023, **33**, 2213510.
21 Y. Wang, R. Zhao, M. Liu, J. Yang, A. Zhang, J. Yue, C. Wu and Y. Bai, *Adv. Energy Mater.*, 2023, **13**, 2302707.

22 J. Shi, T. Sun, J. Bao, S. Zheng, H. Du, L. Li, X. Yuan, T. Ma and Z. Tao, *Adv. Funct. Mater.*, 2021, **31**, 2102035.
23 C. M. Rost, E. Sachet, T. Borman, A. Moballegh, E. C. Dickey, D. Hou, J. L. Jones, S. Curtarolo and J. P. Maria, *Nat. Commun.*, 2015, **6**, 8485.
24 Y. Dang, Z. Xu, Y. Wu, R. Zheng, Z. Wang, X. Lin, Y. Liu, Z. Y. Li, K. Sun, D. Chen and D. Wang, *J. Energy Chem.*, 2024, **95**, 577–587.
25 X. Han, F. Wu, R. Zhao, Y. Bai and C. Wu, *ACS Appl. Mater. Interfaces*, 2023, **15**, 6888–6901.
26 D. Bérardan, S. Franger, D. Dragoe, A. K. Meena and N. Dragoe, *Phys. Status Solidi RRL*, 2016, **10**, 328–333.
27 B. Cantor, I. T. H. Chang, P. Knight and A. J. B. Vincent, *Mater. Sci. Eng., A*, 2004, **375**, 213–218.
28 J. W. Yeh, S. K. Chen, S. J. Lin, J. Y. Gan, T. S. Chin, T. T. Shun, C. H. Tsau and S. Y. Chang, *Adv. Eng. Mater.*, 2004, **6**, 299–303.
29 J. Liang, G. Cao, M. Zeng and L. Fu, *Chem. Soc. Rev.*, 2024, **53**, 6021–6041.
30 J. W. Yeh, *JOM*, 2013, **65**, 1759–1771.
31 J. Su, Z. Cao, Z. Jiang, G. Chen, Y. Zhu, L. Wang and G. Li, *Int. J. Appl. Ceram. Technol.*, 2022, **19**, 2004–2015.
32 M. Fu, X. Ma, K. Zhao, X. Li and D. Su, *iScience*, 2021, **24**, 102177.
33 D. B. Miracle and O. N. Senkov, *Acta Mater.*, 2017, **122**, 448–511.
34 T. X. Nguyen, C. C. Tsai, J. Patra, O. Clemens, J. K. Chang and J. M. Ting, *Chem. Eng. J.*, 2022, **430**, 132658.
35 R. Zhang, C. Wang, P. Zou, R. Lin, L. Ma, L. Yin, T. Li, W. Xu, H. Jia, Q. Li, S. Sainio, K. Kisslinger, S. E. Trask, S. N. Ehrlich, Y. Yang, A. M. Kiss, M. Ge, B. J. Polzin, S. J. Lee, W. Xu, Y. Ren and H. L. Xin, *Nature*, 2022, **610**, 67–73.
36 E. P. George, D. Raabe and R. O. Ritchie, *Nat. Rev. Mater.*, 2019, **4**, 515–534.
37 H. Li, M. Xu, H. Long, J. Zheng, L. Zhang, S. Li, C. Guan, Y. Lai and Z. Zhang, *Adv. Sci.*, 2022, **9**, e2202082.
38 D. Wang, S. Jiang, C. Duan, J. Mao, Y. Dong, K. Dong, Z. Wang, S. Luo, Y. Liu and X. Qi, *J. Alloys Compd.*, 2020, **844**, 156158.
39 H. Z. Xiang, H. X. Xie, Y. X. Chen, H. Zhang, A. Mao and C.-H. Zheng, *J. Mater. Sci.*, 2021, **56**, 8127–8142.
40 B. Xiao, G. Wu, T. Wang, Z. Wei, Y. Sui, B. Shen, J. Qi, F. Wei and J. Zheng, *Nano Energy*, 2022, **95**, 106962.
41 Z. Y. Gu, J. Z. Guo, J. M. Cao, X. T. Wang, X. X. Zhao, X. Y. Zheng, W. H. Li, Z. H. Sun, H. J. Liang and X. L. Wu, *Adv. Mater.*, 2022, **34**, e2110108.
42 K. Tian, H. He, X. Li, D. Wang, Z. Wang, R. Zheng, H. Sun, Y. Liu and Q. Wang, *J. Mater. Chem. A*, 2022, **10**, 14943–14953.
43 J. Zhao, Y. Zhang, X. Chen, G. Sun, X. Yang, Y. Zeng, R. Tian and F. Du, *Adv. Funct. Mater.*, 2022, **32**, 2206531.
44 C. Zhao, F. Ding, Y. Lu, L. Chen and Y. S. Hu, *Angew. Chem., Int. Ed.*, 2020, **59**, 264–269.
45 Y. Ma, Y. Ma, S. L. Dreyer, Q. Wang, K. Wang, D. Goonetilleke, A. Omar, D. Mikhailova, H. Hahn, B. Breitung and T. Brezesinski, *Adv. Mater.*, 2021, **33**, 2101342.
46 Z. Wang, H. Ge, S. Liu, G. Li and X. Gao, *Energy Environ. Mater.*, 2023, **6**, e12358.
47 M. Du, P. Geng, C. Pei, X. Jiang, Y. Shan, W. Hu, L. Ni and H. Pang, *Angew. Chem., Int. Ed.*, 2022, **61**, e202209350.
48 L. Tian, Z. Zhang, S. Liu, G. Li and X. Gao, *Energy Environ. Mater.*, 2021, **5**, 645–654.
49 G. Fang, J. Gao, J. Lv, H. Jia, H. Li, W. Liu, G. Xie, Z. Chen, Y. Huang, Q. Yuan, X. Liu, X. Lin, S. Sun and H. J. Qiu, *Appl. Catal., B*, 2020, **268**, 118431.
50 R. K. Nutor, Q. Cao, R. Wei, Q. Su, G. Du, X. Wang, F. Li, D. Zhang and J. Z. Jiang, *Sci. Adv.*, 2021, **7**, eabi4404.
51 S. Sun, Z. Han, W. Liu, Q. Xia, L. Xue, X. Lei, T. Zhai, D. Su and H. Xia, *Nat. Commun.*, 2023, **14**, 6662.
52 W. Zheng, G. Liang, Q. Liu, J. Li, J. A. Yuwono, S. Zhang, V. K. Peterson and Z. Guo, *Joule*, 2023, **7**, 2732–2748.
53 A. Sarkar, B. Breitung and H. Hahn, *Scr. Mater.*, 2020, **187**, 43–48.
54 T. X. Nguyen, J. Patra, J. K. Chang and J. M. Ting, *J. Mater. Chem. A*, 2020, **8**, 18963–18973.
55 A. Sarkar, Q. Wang, A. Schiele, M. R. Chellali, S. S. Bhattacharya, D. Wang, T. Brezesinski, H. Hahn, L. Velasco and B. Breitung, *Adv. Mater.*, 2019, **31**, 1806236.
56 P. Ghigna, L. Airoldi, M. Fracchia, D. Callegari, U. Anselmi-Tamburini, P. D'Angelo, N. Pianta, R. Ruffo, G. Cibin, D. O. de Souza and E. Quartarone, *ACS Appl. Mater. Interfaces*, 2020, **12**, 50344–50354.
57 A. Mao, H. Z. Xiang, Z. G. Zhang, K. Kuramoto, H. Zhang and Y. Jia, *J. Magn. Magn. Mater.*, 2020, **497**, 165884.
58 H. Minouei, N. Tsvetkov, M. Kheradmandfard, J. Han, D. E. Kim and S. I. Hong, *J. Power Sources*, 2022, **549**, 232041.
59 X. Li, Z. Qiang, G. Han, S. Guan, Y. Zhao, S. Lou and Y. Zhu, *Nano-Micro Lett.*, 2023, **16**, 55.
60 L. Lin, K. Wang, A. Sarkar, C. Njel, G. Karkera, Q. Wang, R. Azmi, M. Fichtner, H. Hahn, S. Schweidler and B. Breitung, *Adv. Energy Mater.*, 2022, **12**, 2103090.
61 Y. Ma, Y. Ma, Q. Wang, S. Schweidler, M. Botros, T. Fu, H. Hahn, T. Brezesinski and B. Breitung, *Energy Environ. Sci.*, 2021, **14**, 2883–2905.
62 Y. Chen, H. Fu, Y. Huang, L. Huang, X. Zheng, Y. Dai, Y. Huang and W. Luo, *ACS Mater. Lett.*, 2020, **3**, 160–170.
63 Q. Wang, A. Sarkar, D. Wang, L. Velasco, R. Azmi, S. S. Bhattacharya, T. Bergfeldt, A. Düvel, P. Heitjans, T. Brezesinski, H. Hahn and B. Breitung, *Energy Environ. Sci.*, 2019, **12**, 2433–2442.
64 M. Du, P. Geng, C. Pei, X. Jiang, Y. Shan, W. Hu, L. Ni and H. Pang, *Angew. Chem., Int. Ed.*, 2022, **61**, e202209350.
65 Y. Ma, Y. Hu, Y. Pramudya, T. Diemant, Q. Wang, D. Goonetilleke, Y. Tang, B. Zhou, H. Hahn, W. Wenzel, M. Fichtner, Y. Ma, B. Breitung and T. Brezesinski, *Adv. Funct. Mater.*, 2022, **32**, 2202372.
66 H. Guo, J. Shen, T. Wang, C. Cheng, H. Yao, X. Han and Q. Zheng, *Ceram. Int.*, 2022, **48**, 3344–3350.
67 C. Y. He, Y. Li, Z. H. Zhou, B. H. Liu and X. H. Gao, *Adv. Mater.*, 2024, **36**, 2400920.

68 X. Chang, M. Zeng, K. Liu and L. Fu, *Adv. Mater.*, 2020, **32**, 1907226.
69 P. Kumari, A. K. Gupta, R. K. Mishra, M. Ahmad and R. R. Shahi, *J. Magn. Magn. Mater.*, 2022, **554**, 169142.
70 X. Wang, W. Guo and Y. Fu, *J. Mater. Chem. A*, 2021, **9**, 663–701.
71 X. Wang, X. Li, H. Fan, M. Miao, Y. Zhang, W. Guo and Y. Fu, *J. Energy Chem.*, 2022, **67**, 276–289.
72 Y. Ye, Q. Wang, J. Lu, C. Liu and Y. J. M. T. Yang, *Mater. Today*, 2016, **19**, 349–362.
73 Y. Zhao, S. Zhang, Y. Zhang, J. Liang, L. Ren, H. J. Fan, W. Liu and X. Sun, *Energy Environ. Sci.*, 2024, **17**, 1279–1290.
74 R. J. Spurling, E. A. Lass, X. Wang and K. Page, *Phys. Rev. Mater.*, 2022, **6**, 090301.
75 J. Yue, S. Chen, J. Yang, S. Li, G. Tan, R. Zhao, C. Wu and Y. Bai, *Adv. Mater.*, 2024, **36**, 2304040.
76 J. Liang, J. Liu, H. Wang, Z. Li, G. Cao, Z. Zeng, S. Liu, Y. Guo, M. Zeng and L. Fu, *J. Am. Chem. Soc.*, 2024, **146**, 7118–7123.
77 N. Qiu, H. Chen, Z. Yang, S. Sun, Y. Wang and Y. Cui, *J. Alloys Compd.*, 2019, **777**, 767–774.
78 H. Chen, N. Qiu, B. Wu, Z. Yang, S. Sun and Y. Wang, *RSC Adv.*, 2020, **10**, 9736–9744.
79 A. Mao, H. X. Xie, H. Z. Xiang, Z. G. Zhang, H. Zhang and S. Ran, *J. Magn. Magn. Mater.*, 2020, **503**, 166594.
80 A. Mao, H.-Z. Xiang, Z. G. Zhang, K. Kuramoto, H. Yu and S. Ran, *J. Magn. Magn. Mater.*, 2019, **484**, 245–252.
81 J. Patra, T. X. Nguyen, C. C. Tsai, O. Clemens, J. Li, P. Pal, W. K. Chan, C. H. Lee, H. Y. T. Chen, J. M. Ting and J. K. Chang, *Adv. Funct. Mater.*, 2022, **32**, 2110992.
82 S. C. Kim, J. Wang, R. Xu, P. Zhang, Y. Chen, Z. Huang, Y. Yang, Z. Yu, S. T. Oyakhire, W. Zhang, L. C. Greenburg, M. S. Kim, D. T. Boyle, P. Sayavong, Y. Ye, J. Qin, Z. Bao and Y. Cui, *Nat. Energy*, 2023, **8**, 814–826.
83 Y. Li, S. Song, H. Kim, K. Nomoto, H. Kim, X. Sun, S. Hori, K. Suzuki, N. Matsui, M. Hirayama, T. Mizoguchi, T. Saito, T. Kamiyama and R. Kanno, *Science*, 2023, **381**, 50–53.
84 J. Yue, S. Li, S. Chen, J. Yang, X. Lu, Y. Li, R. Zhao, C. Wu and Y. Bai, *Energy Mater. Adv.*, 2023, **4**, 0050.
85 Z. Tang, W. Chen, Z. Lyu and Q. Chen, *Energy Mater. Adv.*, 2022, 9765710.
86 W. Li, B. Song and A. Manthiram, *Chem. Soc. Rev.*, 2017, **46**, 3006–3059.
87 F. Wang, X. Wu, C. Li, Y. Zhu, L. Fu, Y. Wu and X. Liu, *Energy Environ. Sci.*, 2016, **9**, 3570–3611.
88 W. Li, E. M. Erickson and A. Manthiram, *Nat. Energy*, 2020, **5**, 26–34.
89 S. Lee, L. Su, A. Mesnier, Z. Cui and A. Manthiram, *Joule*, 2023, **7**, 2430–2444.
90 S. F. Ng, M. Y. L. Lau and W. J. Ong, *Adv. Mater.*, 2021, **33**, 2008654.
91 Y. Zheng, Y. Yi, M. Fan, H. Liu, X. Li, R. Zhang, M. Li and Z.-A. Qiao, *Energy Storage Mater.*, 2019, **23**, 678–683.
92 Y. Cui, P. A. Sukkurji, K. Wang, R. Azmi, A. M. Nunn, H. Hahn, B. Breitung, Y. Y. Ting, P. M. Kowalski, P. Kaghazchi, Q. Wang, S. Schweidler and M. Botros, *J. Energy Chem.*, 2022, **72**, 342–351.
93 L. Tian, Z. Zhang, S. Liu, G. Li and X. Gao, *Nano Energy*, 2023, **106**, 108037.
94 H. Xu, R. Hu, Y. Zhang, H. Yan, Q. Zhu, J. Shang, S. Yang and B. Li, *Energy Storage Mater.*, 2021, **43**, 212–220.
95 G. G. Amatucci and N. Pereira, *J. Fluorine Chem.*, 2007, **128**, 243–262.
96 L. Fang, H. Li, B. B. Xu, J. Ma, H. Pan, Q. He, T. Zheng, W. Ni, Y. Lin, Y. Li, Y. Cao, C. Sun, M. Yan, W. Sun and Y. Jiang, *Small*, 2022, **18**, 2204912.
97 S. Chu, S. Guo and H. Zhou, *Chem. Soc. Rev.*, 2021, **50**, 13189–13235.
98 Y. You, X.-L. Wu, Y.-X. Yin and Y.-G. Guo, *Energy Environ. Sci.*, 2014, **7**, 1643–1647.
99 M. Yuan, H. Liu and F. Ran, *Mater. Today*, 2023, **63**, 360–379.
100 Q. Wang, D. Zhou, C. Zhao, J. Wang, H. Guo, L. Wang, Z. Yao, D. Wong, G. Schuck, X. Bai, J. Lu and M. Wagemaker, *Nat. Sustain.*, 2024, **7**, 338–347.
101 Y. Zhao, Q. Liu, X. Zhao, D. Mu, G. Tan, L. Li, R. Chen and F. Wu, *Mater. Today*, 2023, **62**, 271–295.
102 J. Qian, C. Wu, Y. Cao, Z. Ma, Y. Huang, X. Ai and H. Yang, *Adv. Energy Mater.*, 2018, **8**, 1702619.
103 B. Xie, B. Sun, T. Gao, Y. Ma, G. Yin and P. Zuo, *Coord. Chem. Rev.*, 2022, **460**, 214478.
104 Y. Gao, H. Zhang, X. H. Liu, Z. Yang, X. X. He, L. Li, Y. Qiao and S.-L. Chou, *Adv. Energy Mater.*, 2021, **11**, 2101751.
105 N. Voronina and S.-T. Myung, *Energy Mater. Adv.*, 2021, 9819521.
106 L. Zhang, J. Wang, J. Li, G. Schuck, M. Winter, G. Schumacher and J. Li, *Nano Energy*, 2020, **70**, 104535.
107 L. Yao, P. Zou, C. Wang, J. Jiang, L. Ma, S. Tan, K. A. Beyer, F. Xu, E. Hu and H. L. Xin, *Adv. Energy Mater.*, 2022, **12**, 2201989.
108 S. Chu, C. Zhang, H. Xu, S. Guo, P. Wang and H. Zhou, *Angew. Chem., Int. Ed.*, 2021, **60**, 13366–13371.
109 K. Walczak, A. Plewa, C. Ghica, W. Zając, A. Trenczek Zając, M. Zając, J. Toboła and J. Molenda, *Energy Storage Mater.*, 2022, **47**, 500–514.
110 B. Wang, J. Ma, K. Wang, D. Wang, G. Xu, X. Wang, Z. Hu, C.-W. Pao, J.-L. Chen, L. Du, X. Du and G. Cui, *Adv. Energy Mater.*, 2024, 2401090.
111 S. Chu, C. Zhang, H. Xu, S. Guo, P. Wang and H. Zhou, *Angew. Chem., Int. Ed.*, 2021, **60**, 13366–13371.
112 D. Hamani, M. Ati, J. M. Tarascon and P. Rozier, *Electrochem. Commun.*, 2011, **13**, 938–941.
113 C. Zhao, M. Avdeev, L. Chen and Y. S. Hu, *Angew. Chem., Int. Ed.*, 2018, **57**, 7056–7060.
114 Y. Yin, N. Huo, W. Liu, Z. Shi, Q. Wang, Y. Ding, J. Zhang and S. Yang, *Scr. Mater.*, 2016, **110**, 92–95.
115 H. Chen, N. Qiu, B. Wu, Z. Yang, S. Sun and Y. Wang, *RSC Adv.*, 2020, **10**, 9736–9744.
116 M. V. Reddy, G. V. Subba Rao and B. V. R. Chowdari, *Chem. Rev.*, 2013, **113**, 5364–5457.
117 X. Yang, J. Liu, J. Jia, C. Wu, F. Wang, D. Y. Zhu and W. Zeng, *Energy Mater. Adv.*, 2023, **5**, 0089.
118 Y. Huang, X. Zhang, L. Ji, L. Wang, B. B. Xu, M. W. Shahzad, Y. Tang, Y. Zhu, M. Yan, G. Sun and Y. Jiang, *Energy Storage Mater.*, 2023, **58**, 1–8.

119 J. Peng, B. Zhang, W. Hua, Y. Liang, W. Zhang, Y. Du, G. Peleckis, S. Indris, Q. Gu, Z. Cheng, J. Wang, H. Liu, S. Dou and S. Chou, *Angew. Chem., Int. Ed.*, 2023, **62**, e202215865.
120 Z. Y. Gu, J. Z. Guo, J. M. Cao, X. T. Wang, X. X. Zhao, X. Y. Zheng, W. H. Li, Z. H. Sun, H. J. Liang and X. L. Wu, *Adv. Mater.*, 2022, **34**, 2110108.
121 X. Tan, Y. Zhang, S. Xu, P. Yang, T. Liu, D. Mao, J. Qiu, Z. Chen, Z. Lu, F. Pan and W. Chu, *Adv. Energy Mater.*, 2023, **13**, 2300147.
122 S. Chu, C. Shao, J. Tian, J. Wang, Y. Rao, C. Xu, H. Zhou and S. Guo, *ACS Nano*, 2024, **18**, 337–346.
123 G. Zeng, B. Liu, U. Ali, Y. Li, H. Jia, M. Sun, Y. Li, Y. Hao, X. Yong, T. Wang and C. Wang, *Appl. Catal., B*, 2024, **351**, 123996.
124 K. Du, Y. Liu, Y. Zhao, H. Li, H. Liu, C. Sun, M. Han, T. Ma and Y. Hu, *Adv. Mater.*, 2024, e2404172.
125 H. Shuai, R. Liu, W. Li, X. Yang, H. Lu, Y. Gao, J. Xu and K. Huang, *Adv. Energy Mater.*, 2023, **13**, 2202992.
126 J. Liu, Z. Shen and C. Z. Lu, *J. Mater. Chem. A*, 2024, **12**, 2647–2672.
127 Y. Kim, Y. Park, M. Kim, J. Lee, K. J. Kim and J. W. Choi, *Nat. Commun.*, 2022, **13**, 2371.
128 N. Zhang, J. C. Wang, Y. F. Guo, P. F. Wang, Y. R. Zhu and T. F. Yi, *Coord. Chem. Rev.*, 2023, **479**, 215009.
129 H. Chen, C. Dai, F. Xiao, Q. Yang, S. Cai, M. Xu, H. J. Fan and S. J. Bao, *Adv. Mater.*, 2022, **34**, 2109092.
130 H. g Wang, Q. Wu, L. Cheng and G. Zhu, *Coord. Chem. Rev.*, 2022, **472**, 214772.
131 W. Qu, Y. Cai, B. Chen and M. Zhang, *Energy Environ. Mater.*, 2024, **7**, e12645.
132 Y. Xu, G. Fan, P. X. Sun, Y. Guo, Y. Wang, X. Gu, L. Wu and L. Yu, *Angew. Chem., Int. Ed.*, 2023, **62**, e202303529.
133 S. Shen, D. Ma, K. Ouyang, Y. Chen, M. Yang, Y. Wang, S. Sun, H. Mi, L. Sun, C. He and P. Zhang, *Adv. Funct. Mater.*, 2023, **33**, 2304255.
134 C. Zuo, F. Chao, M. Li, Y. Dai, J. Wang, F. Xiong, Y. Jiang and Q. An, *Adv. Energy Mater.*, 2023, **13**, 2301014.
135 K. Du, Y. Liu, Y. Yang, F. Cui, J. Wang, M. Han, J. Su, J. Wang, X. Han and Y. Hu, *Adv. Mater.*, 2023, **35**, 2301538.
136 Z. Fan, J. Wang, Y. Wu, X. Yan, D. Dai and X. L. Wu, *J. Energy Chem.*, 2024, **97**, 237–264.
137 F. Zhang, M. Du, Z. Miao, H. Li, W. Dong, Y. Sang, H. Jiang, W. Li, H. Liu and S. Wang, *InfoMat*, 2022, **4**, e12346.
138 L. Ni, H. Chen, J. Gao, Y. Mei, H. Wang, F. Zhu, J. Huang, B. Zhang, W. Xu, B. Song, Y. Zhang, W. Deng, G. Zou, H. Hou, Y. Zhou and X. Ji, *Nano Energy*, 2023, **115**, 108743.
139 H. Wang, X. Gao, S. Zhang, Y. Mei, L. Ni, J. Gao, H. Liu, N. Hong, B. Zhang, F. Zhu, W. Deng, G. Zou, H. Hou, X. Y. Cao, H. Chen and X. Ji, *ACS Nano*, 2023, **17**, 12530–12543.
140 G. Zeng, B. Liu, U. Ali, Y. Li, H. Jia, M. Sun, Y. Li, Y. Hao, X. Yong, T. Wang and C. Wang, *Appl. Catal., B*, 2024, **351**, 123996.
141 T. F. Yi, L. Qiu, J. P. Qu, H. Liu, J. H. Zhang and Y. R. Zhu, *Coord. Chem. Rev.*, 2021, **446**, 214124.
142 H. Hu, C. Yang, F. Chen, J. Li, X. Jia, Y. Wang, X. Zhu, Z. Man, G. Wu and W. Chen, *Adv. Mater.*, 2024, **36**, 2406483.
143 B. Wang, J. Ma, K. Wang, D. Wang, G. Xu, X. Wang, Z. Hu, C.-W. Pao, J.-L. Chen, L. Du, X. Du and G. Cui, *Adv. Energy Mater.*, 2024, **14**, 2401090.
144 Y. Ma, Y. Ma, S. L. Dreyer, Q. Wang, K. Wang, D. Goonetilleke, A. Omar, D. Mikhailova, H. Hahn, B. Breitung and T. Brezesinski, *Adv. Mater.*, 2021, **33**, e2101342.
145 G. Li, L. Sun, S. Zhang, C. Zhang, H. Jin, K. Davey, G. Liang, S. Liu, J. Mao and Z. Guo, *Adv. Funct. Mater.*, 2024, **34**, 2301291.
146 Z. Hou, J. Wang, N. Dai, S. Yao, S. Wang, Y. Ji, X. Gao, H. Zhang, Z. Tang, Y. Sun, S. Li, Y. Liu, W. Fu, K. Nie, Y. Jiang, Y.-M. Yan and Z. Yang, *Adv. Energy Mater.*, 2024, **14**, 2302477.
147 P. Byeon, Y. Hong, H. B. Bae, J. Shin, J. W. Choi and S. Y. Chung, *Nat. Commun.*, 2021, **12**, 4599.
148 S. Zhu, W. Nong, L. J. J. Nicholas, X. Cao, P. Zhang, Y. Lu, M. Xiu, K. Huang, G. Wu, S. W. Yang, J. Wu, Z. Liu, M. Srinivasan, K. Hippalgaonkar and Y. Huang, *J. Mater. Chem. A*, 2024, **12**, 11473–11486.
149 H. Yang, L. He, Q. Chen, J. Zhu, G. Jiang, N. Qiu and Y. Wang, *Chem. Eng. J.*, 2024, **488**, 151113.
150 Z. Rák, J. P. Maria and D. W. Brenner, *Mater. Lett.*, 2018, **217**, 300–303.
151 H. Wang, Q. He, X. Gao, Y. Shang, W. Zhu, W. Zhao, Z. Chen, H. Gong and Y. Yang, *Adv. Mater.*, 2024, **36**, 2305453.
152 X. Tan, Y. Zhang, S. Xu, P. Yang, T. Liu, D. Mao, J. Qiu, Z. Chen, Z. Lu, F. Pan and W. Chu, *Adv. Energy Mater.*, 2023, **13**, 2300147.
153 W. L. Hsu, C.-W. Tsai, A. C. Yeh and J. W. Yeh, *Nat. Rev. Chem.*, 2024, **8**, 471–485.
154 Y. Yao, Q. Dong, A. Brozena, J. Luo, J. Miao, M. Chi, C. Wang, I. G. Kevrekidis, Z. J. Ren, J. Greeley, G. Wang, A. Anapolsky and L. Hu, *Science*, 2022, **376**, eabn3103.
155 A. Laha, S. Yoshida, F. Marques dos Santos Vieira, H. Yi, S. H. Lee, S. V. G. Ayyagari, Y. Guan, L. Min, J. Gonzalez Jimenez, L. Miao, D. Graf, S. Sarker, W. Xie, N. Alem, V. Gopalan, C.-Z. Chang, I. Dabo and Z. Mao, *Nat. Commun.*, 2024, **15**, 3532.
156 F. Ding, P. Ji, Z. Han, X. Hou, Y. Yang, Z. Hu, Y. Niu, Y. Liu, J. Zhang, X. Rong, Y. Lu, H. Mao, D. Su, L. Chen and Y. S. Hu, *Nat. Energy*, 2024, 1–11.
157 X. Kong, R. Gu, Z. Jin, L. Zhang, C. Zhang, W. Xiang, C. Li, K. Zhu, Y. Xu, H. Huang, X. Liu, R. Peng and C. Wang, *Nat. Commun.*, 2024, **15**, 7247.
158 D. Wang, S. Jiang, C. Duan, J. Mao, Y. Dong, K. Dong, Z. Wang, S. Luo, Y. Liu and X. Qi, *J. Alloys Compd.*, 2020, **844**, 156158.
159 Y. Zhu, L. Zhang, B. Zhao, H. Chen, X. Liu, R. Zhao, X. Wang, J. Liu, Y. Chen and M. Liu, *Adv. Funct. Mater.*, 2019, **29**, 1901783.
160 E. Lökçü, Ç. Toparli and M. Anik, *ACS Appl. Mater. Interfaces*, 2020, **12**, 23860–23866.

161 Y. Li, X. Li, H. Duan, S. Xie, R. Dai, J. Rong, F. Kang and L. Dong, *Chem. Eng. J.*, 2022, **441**, 136008.
162 N. Mahmood, T. Tang and Y. Hou, *Adv. Energy Mater.*, 2016, **6**, 1600374.
163 D. Chen, J. Ahn and G. Chen, *ACS Energy Lett.*, 2021, **6**, 1358–1376.
164 K. H. Nam, S. Jeong, B. C. Yu, J. H. Choi, K. J. Jeon and C. M. Park, *ACS Nano*, 2022, **16**, 13704–13714.
165 Y. Lu, L. Yu and X. W. Lou, *Chem*, 2018, **4**, 972–996.
166 K. Wang, W. Hua, X. Huang, D. Stenzel, J. Wang, Z. Ding, Y. Cui, Q. Wang, H. Ehrenberg, B. Breitung, C. Kubel and X. Mu, *Nat. Commun.*, 2023, **14**, 1487.
167 A. Sarkar, L. Velasco, D. Wang, Q. Wang, G. Talasila, L. de Biasi, C. Kübel, T. Brezesinski, S. S. Bhattacharya, H. Hahn and B. Breitung, *Nat. Commun.*, 2018, **9**, 3400.
168 J. Wei, K. Rong, X. Li, Y. Wang, Z. A. Qiao, Y. Fang and S. Dong, *Nano Res.*, 2022, **15**, 2756–2763.
169 D. Csík, D. Zalka, K. Saksl, D. Capková and R. Džunda, *J. Phys.: Conf. Ser.*, 2022, **2382**, 012003.
170 Q. Wang, A. Sarkar, Z. Li, Y. Lu, L. Velasco, S. S. Bhattacharya, T. Brezesinski, H. Hahn and B. Breitung, *Electrochem. Commun.*, 2019, **100**, 121–125.
171 G. Yu, Q. Zhang, J. Jing, X. Wang, Y. Li, X. Bai and T. Li, *Small*, 2023, **19**, 2303087.
172 W. Li, J.-H. Wang, L. Yang, Y. Li, H.-Y. Yen, J. Chen, L. He, Z. Liu, P. Yang, Z. Guo and M. Liu, *Adv. Mater.*, 2024, **36**, 2314054.
173 X. Liu, X. Li, Y. Li, H. Zhang, Q. Jia, S. Zhang and W. Lei, *EcoMat*, 2022, **4**, e12261.
174 W. Wang, W. Song, Y. Li, Y. Guo, K. Yang, L. Yu, F. Xie, Q. Ren, K. He, S. Wang and Y. Yuan, *Nano Energy*, 2024, **124**, 109482.
175 P. Ghigna, L. Airoldi, M. Fracchia, D. Callegari, U. Anselmi-Tamburini, P. D'Angelo, N. Pianta, R. Ruffo, G. Cibin, D. O. de Souza and E. Quartarone, *ACS Appl. Mater. Interfaces*, 2020, **12**, 50344–50354.
176 X. Liu, Y. Xing, K. Xu, H. Zhang, M. Gong, Q. Jia, S. Zhang and W. Lei, *Small*, 2022, **18**, 2200524.
177 J. Zhao, X. Yang, Y. Huang, F. Du and Y. Zeng, *ACS Appl. Mater. Interfaces*, 2021, **13**, 58674–58681.
178 R. Wei, K. Zhang, P. Zhao, Y. An, C. Tang, C. Chen, X. Li, X. Ma, Y. Ma and X. Hao, *Appl. Surf. Sci.*, 2021, **549**, 149327.
179 K. Gu, D. Wang, C. Xie, T. Wang, G. Huang, Y. Liu, Y. Zou, L. Tao and S. Wang, *Angew. Chem., Int. Ed.*, 2021, **60**, 20253–20258.
180 H. Minouei, N. Tsvetkov, M. Kheradmandfard, J. Han, D.-E. Kim and S. I. Hong, *J. Power Sources*, 2022, **549**, 232041.
181 S. Hou, L. Su, S. Wang, Y. Cui, J. Cao, H. Min, J. Bao, Y. Shen, Q. Zhang, Z. Sun, C. Zhu, J. Chen, Q. Zhang and F. Xu, *Adv. Funct. Mater.*, 2023, **34**, 2307923.
182 X. Wang, G. Liu, C. Tang, H. Tang, W. Zhang, Z. Ju, J. Jiang, Q. Zhuang and Y. Cui, *J. Alloys Compd.*, 2023, **934**, 167889.
183 W. Li, J. H. Wang, Y. Li, H. Hsueh, X. Liu, Y. Zhao, S. Huang, X. Li, H.-M. Cheng, X. Duan and H. S. Park, *J. Am. Chem. Soc.*, 2024, **146**, 21320–21334.
184 X. W. Yang, X. H. Shi, H. J. Yang, J. W. Qiao, P. K. Liaw and Y. C. Wu, *Rare Met.*, 2022, **41**, 2906–2920.
185 Y. Wei, X. Liu, R. Yao, J. Qian, Y. Yin, D. Li and Y. Chen, *J. Alloys Compd.*, 2023, **938**, 168610.
186 V. Pavlyuk, W. Ciesielski, N. Pavlyuk, D. Kulawik, A. Balińska and K. Kluziak, *Mater.*, 2021, **14**, 4331.
187 J. Wang, Y. Wang, X. Lu, J. Qian, C. Yang, I. Manke, H. Song, J. Liao, S. Wang and R. Chen, *Adv. Mater.*, 2024, **36**, 2308257.
188 J. Liu, Y. Li, Z. Chen, N. Liu, L. Zheng, W. Shi and X. Wang, *J. Am. Chem. Soc.*, 2022, **144**, 23191–23197.
189 S. Qiao, Q. Zhou, M. Ma, H. K. Liu, S. X. Dou and S. Chong, *ACS Nano*, 2023, **17**, 11220–11252.
190 W. Du, E. H. Ang, Y. Yang, Y. Zhang, M. Ye and C. C. Li, *Energy Environ. Sci.*, 2020, **13**, 3330–3360.
191 C. Xie, Y. Li, Q. Wang, D. Sun, Y. Tang and H. Wang, *Carbon Energy*, 2020, **2**, 540–560.
192 H. Dong, J. Li, J. Guo, F. Lai, F. Zhao, Y. Jiao, D. J. L. Brett, T. Liu, G. He and I. P. Parkin, *Adv. Mater.*, 2021, **33**, 2007548.
193 M. Yao, Z. Yuan, S. Li, T. He, R. Wang, M. Yuan and Z. Niu, *Adv. Mater.*, 2021, **33**, 2008140.
194 Y. Li, Z. Wang, Y. Cai, M. E. Pam, Y. Yang, D. Zhang, Y. Wang and S. Huang, *Energy Environ. Mater.*, 2022, **5**, 823–851.
195 G. Fang, J. Zhou, A. Pan and S. Liang, *ACS Energy Lett.*, 2018, **3**, 2480–2501.
196 Y. Zhu, J. Yin, X. Zheng, A. H. Emwas, Y. Lei, O. F. Mohammed, Y. Cui and H. N. Alshareef, *Energy Environ. Sci.*, 2021, **14**, 4463–4473.
197 Y. Tian, Y. An, C. Wei, B. Xi, S. Xiong, J. Feng and Y. Qian, *Adv. Energy Mater.*, 2021, **11**, 2002529.
198 Y. Zhu, G. Liang, X. Cui, X. Liu, H. Zhong, C. Zhi and Y. Yang, *Energy Environ. Sci.*, 2024, **17**, 369–385.
199 Z. Feng, Y. Feng, F. Fan, D. Deng, H. Dong, S. Liu, L. Kang, S. C. Jun, L. Wang, J. Zhu, L. Dai and Z. He, *SusMat*, 2024, **4**, e184.
200 S. Xie, Y. Li and L. Dong, *J. Energy Chem.*, 2023, **76**, 32–40.
201 B. Liu, S. Wang, Z. Wang, H. Lei, Z. Chen and W. Mai, *Small*, 2020, **16**, 2001323.
202 Y. Chen, Q. Zhao, Y. Wang, W. Liu, P. Qing and L. Chen, *Electrochim. Acta*, 2021, **399**, 139334.
203 D. Han, S. Wu, S. Zhang, Y. Deng, C. Cui, L. Zhang, Y. Long, H. Li, Y. Tao, Z. Weng, Q.-H. Yang and F. Kang, *Small*, 2020, **16**, 2001736.
204 Z. Qi, T. Xiong, T. Chen, C. Yu, M. Zhang, Y. Yang, Z. Deng, H. Xiao, W. S. V. Lee and J. Xue, *ACS Appl. Mater. Interfaces*, 2021, **13**, 28129–28139.
205 S. B. Wang, Q. Ran, R.-Q. Yao, H. Shi, Z. Wen, M. Zhao, X.-Y. Lang and Q. Jiang, *Nat. Commun.*, 2020, **11**, 1634.
206 Y. Wang, Y. Chen, W. Liu, X. Ni, P. Qing, Q. Zhao, W. Wei, X. Ji, J. Ma and L. Chen, *J. Mater. Chem. A*, 2021, **9**, 8452–8461.
207 J. Luo, L. Xu, Y. Yang, S. Huang, Y. Zhou, Y. Shao, T. Wang, J. Tian, S. Guo, J. Zhao, X. Zhao, T. Cheng, Y. Shao and J. Zhang, *Nat. Commun.*, 2024, **15**, 6471.
208 Y. Du, Y. Feng, R. Li, Z. Peng, X. Yao, S. Duan, S. Liu, S. C. Jun, J. Zhu, L. Dai, Q. Yang, L. Wang and Z. He, *Small*, 2024, **20**, 2307848.

209 T. Wang, Y. Tang, M. Yu, B. Lu, X. Zhang and J. Zhou, *Adv. Funct. Mater.*, 2023, **33**, 2306101.
210 J. Sun, X. Zheng, K. Li, G. Ma, T. Dai, B. Ban, Y. Yuan, M. Wang, M. Chuai, Y. Xu, Z. Liu, T. Jiang, Z. Zhu, J. Chen, H. Hu and W. Chen, *Energy Storage Mater.*, 2023, **54**, 570–578.
211 Y. Chai, X. Xie, Z. He, G. Guo, P. Wang, Z. Xing, B. Lu, S. Liang, Y. Tang and J. Zhou, *Chem. Sci.*, 2022, **13**, 11656–11665.
212 J. Gu, Y. Tao, H. Chen, Z. Cao, Y. Zhang, Z. Du, Y. Cui and S. Yang, *Adv. Energy Mater.*, 2022, **12**, 2200115.
213 G. Q. Liu, B. Fu, Z. X. Liu, L. Y. Li, S. Q. Liang and G. Z. Fang, *Rare Met.*, 2024, 1–12.
214 S. Khamsanga, H. Uyama, W. Nuanwat and P. Pattananuwat, *Sci. Rep.*, 2022, **12**, 8689.
215 J. Xu, P. Han, Y. Jin, H. Lu, B. Sun, B. Gao, T. He, X. Xu, N. Pinna and G. Wang, *ACS Nano*, 2024, **18**, 18592–18603.
216 Y. Xin, J. Qi, H. Xie, Y. Ge, Z. Wang, F. Zhang, B. He, S. Wang and H. Tian, *Adv. Funct. Mater.*, 2024, 2403222.
217 J. Zou, Z. Zeng, C. Wang, X. Zhu, J. Zhang, H. Lan, L. Li, Y. Yu, H. Wang, X. Zhu, Y. Zhang, M. Zeng and L. Fu, *Small Struct.*, 2023, **4**, 2200194.
218 N. Sun, Z. Zheng, Z. Lai, J. Wang, P. Du, T. Ying, H. Wang, J. Xu, R. Yu, Z. Hu, C.-W. Pao, W.-H. Huang, K. Bi, M. Lei and K. Huang, *Adv. Mater.*, 2024, 2404772.
219 Y. Li, H. Jia, U. Ali, H. Wang, B. Liu, L. Li, L. Zhang and C. Wang, *Adv. Energy Mater.*, 2023, **13**, 2301643.
220 L. Zheng, R. Lv, C. Luo, Y. Guo, M. Yang, K. Hu, K. Wang, L. Li, F. Wu and R. Chen, *Adv. Energy Mater.*, 2024, 2402042.
221 Y. Zhang, X. Yang, Y. Hu, K. Hu, X. Lin, X. Liu, K. M. Reddy, G. Xie and H.-J. Qiu, *Small*, 2022, **18**, 2200787.
222 F. Xie, H. Li, X. Wang, X. Zhi, D. Chao, K. Davey and S.-Z. Qiao, *Adv. Energy Mater.*, 2021, **11**, 2003419.
223 C. B. Jin, N. Yao, Y. Xiao, J. Xie, Z. Li, X. Chen, B.-Q. Li, X. Q. Zhang, J. Q. Huang and Q. Zhang, *Adv. Mater.*, 2023, **35**, 2208340.
224 X. Zhao, Z. Fu, X. Zhang, X. Wang, B. Li, D. Zhou and F. Kang, *Energy Environ. Sci.*, 2024, **17**, 2406–2430.
225 M. Li, C. Sun, Q. Ni, Z. Sun, Y. Liu, Y. Li, L. Li, H. Jin and Y. Zhao, *Adv. Energy Mater.*, 2023, **13**, 2203971.
226 Q. Wang, C. Zhao, Z. Yao, J. Wang, F. Wu, S. G. H. Kumar, S. Ganapathy, S. Eustace, X. Bai, B. Li, J. Lu and M. Wagemaker, *Adv. Mater.*, 2023, **31**, 2210677.
227 Y. Zeng, B. Ouyang, J. Liu, Y. W. Byeon, Z. Cai, L. J. Miara, Y. Wang and G. Ceder, *Science*, 2022, **378**, 1320–1324.
228 M. Qiu, P. Sun, K. Han, Z. Pang, J. Du, J. Li, J. Chen, Z. L. Wang and W. Mai, *Nat. Commun.*, 2023, **14**, 601.
229 S. Wang, K. Wang, Y. Zhang, Y. Jie, X. Li, Y. Pan, X. Gao, Q. Nian, R. Cao, Q. Li, S. Jiao and D. Xu, *Angew. Chem., Int. Ed.*, 2023, **31**, e202304411.
230 S. Chai, J. Xia, Y. Li and J. Liu, *Next Energy*, 2024, **2**, 100077.
231 Y. Su, X. Rong, H. Li, X. Huang, L. Chen, B. Liu and Y. S. Hu, *Adv. Mater.*, 2023, **35**, 2209402.
232 Z. Song, T. Wang, H. Yang, W. H. Kan, Y. Chen, Q. Yu, L. Wang, Y. Zhang, Y. Dai, H. Chen, W. Yin, T. Honda, M. Avdeev, H. Xu, J. Ma, Y. Huang and W. Luo, *Nat. Commun.*, 2024, **15**, 1481.
233 C. Yang, J. Xia, C. Cui, T. P. Pollard, J. Vatamanu, A. Faraone, J. A. Dura, M. Tyagi, A. Kattan, E. Thimsen, J. Xu, W. Song, E. Hu, X. Ji, S. Hou, X. Zhang, M. S. Ding, S. Hwang, D. Su, Y. Ren, X.-Q. Yang, H. Wang, O. Borodin and C. Wang, *Nat. Sustain.*, 2023, **6**, 325–335.
234 H. Yan, X. Zhang, Z. Yang, M. Xia, C. Xu, Y. Liu, H. Yu, L. Zhang and J. Shu, *Coord. Chem. Rev.*, 2022, **452**, 214297.
235 L. Sheng, Y. Wu, J. Tian, L. Wang, J. Wang, Y. Tang, H. Xu and X. He, *Energy Environ. Mater.*, 2023, **6**, e12266.
236 D. Han, T. Sun, R. Zhang, W. Zhang, T. Ma, H. Du, Q. Wang, D. He, S. Zheng and Z. Tao, *Adv. Funct. Mater.*, 2022, **32**, 2209065.
237 X. Bai, M. Sun, J. Yang, B. Deng, K. Yang, B. Huang, W. Hu and X. Pu, *Energy Environ. Sci.*, 2024, **17**, 7330–7341.
238 L. E. Blanc, D. Kundu and L. F. Nazar, *Joule*, 2020, **4**, 771–799.
239 H. Jia, X. Jiang, Y. Wang, Y. Lam, S. Shi and G. Liu, *Adv. Energy Mater.*, 2024, **14**, 2304285.
240 Q. Wang, C. Zhao, Z. Yao, J. Wang, F. Wu, S. G. H. Kumar, S. Ganapathy, S. Eustace, X. Bai, B. Li, J. Lu and M. Wagemaker, *Adv. Mater.*, 2023, **35**, 2210677.
241 M. Wang, M. Zheng, J. Lu and Y. You, *Joule*, 2024, **9**, 2467–2482.
242 C. Huang, D. Zhu, X. Zhao, Y. Hao, Y. Yang, Y. Qian, G. Chang, Q. Tang, A. Hu and X. Chen, *Angew. Chem., Int. Ed.*, 2024, e202411427.
243 H. Raza, J. Cheng, C. Lin, S. Majumder, G. Zheng and G. Chen, *EcoMat*, 2023, **5**, e12324.
244 Y. Li, X. Bai, D. Yuan, C. Yu, X. San, Y. Guo, L. Zhang and J. Ye, *Nat. Commun.*, 2023, **14**, 3171.
245 Q. Wang, C. Zhao, J. Wang, Z. Yao, S. Wang, S. G. H. Kumar, S. Ganapathy, S. Eustace, X. Bai, B. Li and M. Wagemaker, *Nat. Commun.*, 2023, **14**, 440.
246 L. Banko, E. B. Tetteh, A. Kostka, T. H. Piotrowiak, O. A. Krysiak, U. Hagemann, C. Andronescu, W. Schuhmann and A. Ludwig, *Adv. Mater.*, 2023, **35**, 2207635.
247 T. Cai, M. Cai, J. Mu, S. Zhao, H. Bi, W. Zhao, W. Dong and F. Huang, *Nano-Micro Lett.*, 2023, **16**, 10.
248 W. Zhang, H. Xia, Z. Zhu, Z. Lv, S. Cao, J. Wei, Y. Luo, Y. Xiao, L. Liu and X. Chen, *CCS Chem.*, 2020, **3**, 1245–1255.
249 Y. T. Yeh, C. W. Huang, A. Y. Hou, C. Y. Huang, Y. D. Lin and W. W. Wu, *Small*, 2024, **20**, 2307284.
250 W. Jiang, T. Wang, H. Chen, X. Suo, J. Liang, W. Zhu, H. Li and S. Dai, *Nano Energy*, 2021, **79**, 105464.
251 C. B. Chang, Y. R. Lu and H. Y. Tuan, *Energy Storage Mater.*, 2023, **59**, 102770.